homologous globular lobes (an N-lobe and a C-lobe), each with a single iron (Fe^{3+}) binding site. There is a notable degree of internal homology between the two lobes, *i.e.* ~35% identical amino acid residues have been identified in the corresponding portions (26). The three-dimensional structures of human and bovine LFs have been clarified by crystallographic studies (27, 28). Although the overall structure of LF is similar to that of transferrin (TF) (~60% amino acid sequence homology to LF), LF has two distinct features that may be functionally important. First, the association constant of LF for iron is 300 times that of TF (29). Second, in contrast to TF, LF possesses strong inhibitory activity against bacterial growth. The antimicrobial activity of LF has been ascribed to the basic N-terminal region ("lactoferricin") (30). Lactoferricin (24 aa residues) shows activity against a wide range of microorganisms including bacteria and fungi (30). LF is present in the milk of most mammals, and the LF content in milk changes substantially during the lactation period. The concentrations of LF in mature milk are 0.1–0.4 mg/ml in bovines and 1–3 mg/ml in humans, and LF is especially enriched in the colostrum (0.8 mg/ml in bovines and 10 mg/ml in humans) (31, 32). It is well established that LF plays an important role in the newborn as the primary nonspecific defense against pathogenic microorganisms (26). Also, it has been reported that rats fed a 2% bovine LF diet displayed no significant side effects (33). This low risk of severe side effects presents a major clinical advantage of bovine LF; hence, clinical pilot studies have been performed recently. The results have shown that bovine LF was effective in some patients with chronic hepatitis C (34, 35).

A recent study by our group (36) suggested that the prevention of HCV infection in these cells was because of interactions of LF with HCV rather than with the cells themselves; our study demonstrated that LF inhibited viral entry into the cells by interacting directly with HCV (36). On the other hand, Yi *et al.* (37) independently demonstrated that HCV envelope proteins (E1 and E2) could bind to human and bovine LFs, although their binding specificities have not been clarified. E2 protein expressed in mammalian cells specifically binds to human target cells (38), and such binding is associated with HCV particles binding to target cells *in vitro*, as well as with HCV infection *in vivo* (38). In addition, the level of antibody response to E2 protein has been shown to correlate with protection against HCV in animal models (39) and with occasional clearance of HCV in cases of natural infection (40), suggesting that the E2 protein is the major receptor-binding protein. For these reasons, we focused on the interactions between LF and E2 proteins to understand the mechanism by which LF prevents HCV infection of target cells. In this study, we have characterized the binding activity of LF to the E2 protein and have endeavored to determine which region(s) of LF are important for this binding activity. Here, we report the finding of 33 human LF-derived amino acids possessing binding activity to the E2 protein of HCV, which leads to inhibition of HCV infection in target cells.

EXPERIMENTAL PROCEDURES

Far-Western Blot Analysis—Far-Western blot analysis was carried out according to a method described previously (37) with some modifications. Briefly, 0.5 μg of human and bovine LFs (Sigma) and various recombinant LF fragments were resolved by 10 or 12% SDS-PAGE and were transferred to polyvinylidene difluoride membranes. The membranes were then blocked in N-buffer (50 mM Tris, pH 7.5, 150 mM NaCl, 0.1% Triton X-100, 0.25% gelatin) with 2% bovine serum albumin (BSA) for 30 min at room temperature. The binding reaction was carried out at room temperature in N-buffer containing 2% BSA, and the secreted form of E2 protein (E2–681) expressed in Chinese hamster ovary cells was used as a probe (41). After 1 h of incubation, the membranes were washed with N-buffer three times for 10 min at room temperature, blocked once again with N-buffer with 2% BSA, and incubated at room temperature with rat monoclonal antibody, MO-2 or MO-12, against E2 protein (42). Normal rat serum (Invitrogen) was used as a control instead of MO-2 or MO-12. After 1 h of incubation at room temperature, the membranes were washed with 0.1% Tris saline three times for 5 min at room temperature. Immunocomplexes on the membranes were detected by enhanced chemiluminescence assay (Renaissance; PerkinElmer Life Sciences).

Deglycosylation of LF—Human and bovine LFs (10 μg each; Sigma) were denatured with 0.5% SDS, 1% 2-mercaptoethanol for 10 min at 100 °C and were then treated with 2,000 units of peptide-*N*-glycosidase F (PNGaseF; New England Biolabs) in 50 mM sodium phosphate, pH 7.5, 1% Nonidet P-40 for 4 h at 37 °C. After incubation, the samples were immediately used for the Far-Western blot analysis.

Isolation of LF, TF, and CD81 cDNAs—Total RNAs (2 μg each) from human cancer breast tissue (43), normal bovine breast tissue, and normal horse peripheral blood mononuclear cells were used as templates for reverse transcription (RT)-PCR to obtain the full-length LF cDNAs. The total RNA (2 μg) from PH5CH8 cells was also used as a template for RT-PCR to obtain the TF cDNA encoding aa 587–679 and the CD81 cDNA encoding the large extracellular loop (LEL; aa 113–201). Oligo(dT) was used to prime the cDNA synthesis using Superscript II reverse transcriptase (Invitrogen). Amplification by PCR with a highly efficient proofreading DNA polymerase, KOD-plus (Toyobo) was performed for 20 cycles using each primer set (see Table I) arranged from the nucleotide sequences of human LF (X52941), bovine LF (M63502), horse LF (AJ010930), human TF (S95936), and human CD81 (M33680) cDNAs. The PCR product containing the coding region of full-length human LF was cloned into the *Hin*dIII and *Bam*HI sites of the pHook™-2 (Invitrogen), as described previously (44). The PCR products containing the coding region of full-length bovine and horse LFs were also cloned into the *Not*I and *Hpa*I sites of pCXbsr (45), as described previously (46). The PCR products containing the human TF fragment (aa 587–678) and the CD81 LEL were cloned into the *Bam*HI and *Hin*dIII sites of the pET32a (Novagen), respectively. The nucleotide sequences of obtained cDNA clones encoding human, bovine, and horse LF, and human TF and CD81 were determined by Big Dye terminator-cycle sequencing on an Applied Biosystem 310 automated sequencer (Applied Biosystems, Norwalk, CT). It was confirmed that these cDNAs had identical nucleotide sequences to those in the databases.

Construction of Expression Plasmids for Escherichia coli—The pET32a was used for the production of LF, TF, or CD81 fragments as thioredoxin (TRX)-fused proteins in *E. coli*. For the expression of human, bovine, and horse LFs, the inserts of obtained cDNA clones were transferred into the *Bam*HI and *Hin*dIII sites of the pET32a. Based on these pET32a plasmids containing the coding regions of the full-length LFs, the pET32a expression plasmids encoding the various regions of LF were constructed by inserting the PCR product amplified using the primer sets listed in Table I into the *Bam*HI-*Hin*dIII site of the pET32a. The pMAL-c2X (New England Biolabs, Beverly, MA) was used for the production of human LF fragment (aa 600–632) as maltose-binding protein (MBP)-fused protein in *E. coli*. The DNA fragment encoding the human LF fragment (aa 600–632), which was obtained from the pET32a expression vector by digestion with *Bam*HI and *Hin*dIII, was transferred into the *Bam*HI-*Hin*dIII sites of the pMAL-c2X. The single-amino acid substitutions (*i.e.* changed to an Ala residue) were introduced into pET32a containing the coding region of human LF fragment (aa 600–632) by site-directed mutagenesis, as described previously (47), using the mutation primer sets. The obtained pET32a mutants were confirmed by nucleotide sequencing.

Expression and Purification of TRX-fused LF Fragments, TF Fragment, and CD81 LEL—Expression plasmids for TRX-fused human LF fragments were transformed into the *E. coli* strain AD494(DE3) (Novagen). The transformants were cultured in 10 ml of LB medium containing ampicillin (50 μg/ml) and kanamycin (15 μg/ml) at 37 °C overnight and were then transferred to 200 ml of LB medium; the culture period was then for 4 h at 37 °C. One mM isopropyl-β-D-thiogalactopyranoside was added to the culture and then continued for 4–5 h at 37 °C. After centrifugation at 3,400 × *g* for 10 min, the harvested cells were suspended in 10 ml of B-PER™ (Pierce) by pipetting until the cell suspension became homogenous and was incubated for 15 min at room temperature. After centrifugation at 27,000 × *g* for 15 min, the supernatant obtained as the soluble fraction was used for the purification of LF fragments and CD81 LEL using a His-Bind purification kit (Novagen) according to the manufacturer's protocol, because these TRX-fused proteins possesses His tag sequences. On the other hand, the pellets obtained as the insoluble fraction were suspended in 10 ml of B-PER™; 200 μl of lysozyme (10 mg/ml; Sigma) was then added, and the samples were incubated for 5 min at room temperature. After centrifugation at

TABLE I
Oligonucleotides used for construction of expression plasmids

Oligonucleotide	Sequence	Direction	Expressed proteins
hLF(B)	attatGGATCCGGCCGTAGGAGAAGGAGTGTTCAG	Forward	Full-length human LF
hLFCRH	taataAAGCTTTTACTTCCTGAGGAATTCACAGGC	Reverse	Full-length human LF, lactoferricin-truncated human LF, human LF C-lobe and C-s3, human LF (aa 610–692, 624–692, 640–692, 653–692)
hLFB1	tgataGGATCCCAGGCCATTGCGGAAAACAGGGCC	Forward	Lactoferricin-truncated human LF human LF N-lobe and N-s1
hLFH1	taataAAGCTTGGGCTCAGGTGGACCCG	Reverse	Human LF N-s1
hLFB2	tgataGGATCCATTGAGGCAGCTGTGGCCAGGTTC	Forward	Human LF N-s2
hLFH2	taataAAGCTTGGCATGAGAAGGGACCCGGG	Reverse	Human LF N-s2
hLFB3	tgataGGATCCGTTGTGGCACGAAGTGTGTGAATGGC	Forward	Human LF N-s3
hLFNRH	tgataAAGCTTAGCCACTTCCTCCTCACTTTTCCTC	Reverse	Human LF N-lobe and N-s3
hLFCB	tgataGGATCCGCCCGGCGTGCGCGGGTCGTGTGG	Forward	Human LF C-lobe and C-s1
hLFH3	taataAAGGTTAAATTTGCAGGAGCCCGTCTG	Reverse	Human LF C-s1
hLFB5	tgataGGATCCGATGAATATTTCAGTCAAAGCTG	Forward	Human LF C-s2
hLFH4	taataAAGCTTGGCATGATTCGGGGCCATGG	Reverse	Human LF C-s2
hLFB6	tgataGGATCCGTGGTGTCTCGGATGATAAGG	Forward	Human LF C-s3, human LF (aa 600–622, 600–627, 600–632, 600–637, 600–642, 600–647, 600–652, 600–670)
C3ABR	taataAAGCTTTTATGCGACATACTGTGGTCCC	Reverse	Human LF (aa 600–670)
C3ARZ	taataAAGCTTTTAGGCCAGACACTCAGTGTTGTC	Reverse	Human LF (aa 590–652, 600–652, 605–652, 610–652)
C3HF	tgataGGATCCAGACTCCATGGCAAAACAACATATG	Forward	Human LF (aa 653–692)
C3HFA	tgataGGATCCCTGAAACAGGTGCTGCTCCAC	Forward	Human LF (aa 610–692, 610–652)
C3HFB	tgataGGATCCAATGGATCTGACTGCCCGGAC	Forward	Human LF (aa 624–692)
C3HFC	tgataGGATCCAAAAACCTTCTGTTCAATGAC	Forward	Human LF (aa 640–692)
590F	tgataGGATCCCTGCCATCTTGCCATGGCCCCG	Forward	Human LF (aa 590–652)
605F	tgataGGATCCGATAAGGTGGAACGCCTGAAACAGG	Forward	Human LF (aa 605–652, 605–632)
622R	taataAAGCTTTTACCCAAATTTAGCCTGTTGGTGG	Reverse	Human LF (aa 600–622)
627R	taataAAGCTTTTAGTCAGATCCATTTCTCCCAAATTTAGC	Reverse	Human LF (aa 600–627)
632R	taataAAGCTTTTAAAACTTGTCCGGGCAGTCAGATCC	Reverse	Human LF (aa 600–632, 605–632)
637R	taataAAGCTTTTAAGACTGGAATAAGCAAAACTTGTCC	Reverse	Human LF (aa 600–637)
642R	taataAAGCTTTTAAAGGTTTTTGGTTTCAGACTGGAATAA	Reverse	Human LF (aa 600–642)
647R	taataAAGCTTTTAGTTGTCATTGAACAGAAGGTTTTTGG	Reverse	Human LF (aa 600–647)
CD81B	tgataGGATCCTTTGTCAACAAGGACCAG	Forward	Human CD81 LEL (aa 113–201)
CD81RbH	taataAAGCTTCTTCCCGGAGAAGAGGTCATCG	Reverse	Human CD81 LEL (aa 113–201)
bLF(N)	attatGCGGCCGCCACCATGAAGCTCTTCGTCCCCGCCCT	Forward	Full-length bovine LF
bLFR(H)	attatGTTAACTCATTACCTCGTCAGGAAGGCGCAGG	Reverse	Full-length bovine LF
bLFC3F	tgataGGATCCGTGGTGTCTGGAGCGATAGGG	Forward	Bovine LF (aa 597–689, 597–629)
bLFC3R	taataAAGCTTTTACCTCGTCAGGAAGGCGCAGGC	Reverse	Bovine LF (aa 597–689)
bLF632R	taataAAGCTTTTAAAACTTGTCCGGGCAGTTTTTTCC	Reverse	Bovine LF (aa 597–629)
hoLF(N)	attatGCGGCCGCCACCATGGCCCCTAGGAAAAGCGTTCG	Forward	Full-length horse LF
hoLF(H)	attatGTTAACTCATTATGCCCTCAGGAAGGCGCAGGC	Reverse	Full-length horse LF
hoLFC3F	tgataGGATCCGTGGTATCTCAGAGTGATAGGGC	Forward	Horse LF (aa 597–689)
hoLFC3R	taataAAGCTTTTATGCCCTCAGGAAGGCGCAGGC	Reverse	Horse LF (aa 597–689)
C3TF	tgataGGATCCGTGGTCACACGGAAAGATAAGG	Forward	Human TF (aa 587–679)
C3TR	taataAAGCTTTTAAGGTCTACGGAAAGTGCAGGC	Reverse	Human TF (aa 587–679)

27,000 × *g* for 15 min, the pellets were resuspended in 30 ml of 10-fold diluted B-PER™, and the treatment was repeated two times. The pellets obtained by this method were then dissolved in 10 ml of binding buffer (20 mM Tris-HCl, pH 7.9, 500 mM NaCl, 5 mM imidazole, and 6 M urea) as purified inclusion bodies. The inclusion bodies thus obtained were also used for the purification of several LF fragments using a His-Bind purification kit in the presence of 6 M urea. The purity of obtained LF fragments and CD81 LEL was evaluated to be more than 95%, as determined by electrophoresis on 12% SDS-PAGE gels. The protein concentration was determined by using Coomassie protein assay reagent (Pierce). TRX (22 kDa) produced from the pET32a vector, with the linker sequence-derived 26 amino acids in the C-terminal portion, was used as a control protein.

Expression and Purification of the MBP-fused LF Fragment—The expression plasmid for the MBP-fused human LF fragment (aa 600–632) was transformed into the *E. coli* strain JM109. The transformants were cultured in 100 ml of LB medium containing ampicillin (100 μg/ml) and glucose (2 mg/ml) at 37 °C until an optical density of 0.6 at 600 nm was reached. At this point, 1 mM of isopropyl-β-D-thiogalactopyranoside was added to the culture, and the culture was continued for 4 h at 37 °C. After centrifugation at 3,400 × *g* for 10 min, the harvested cells were resuspended in 5 ml of column buffer (20 mM Tris-HCl, pH 7.4, 200 mM NaCl, and 1 mM EDTA) and were then disrupted by sonication for 2 min with short pulses. Insoluble cellular debris was removed by centrifugation at 10,000 × *g* for 30 min at 4 °C. The supernatant obtained as the soluble fraction was applied onto an amylose resin affinity column (New England Biolabs, Beverly, MA). The column was washed with 10 column volumes of column buffer to remove the unbound proteins. The bound protein was eluted with 10 mM maltose under conditions recommended by the manufacturer. The purity of the obtained MBP-fused protein was evaluated to be more than 95% by electrophoresis on 12% SDS-PAGE gels. The concentration of the purified MBP-fused protein was determined by using Coomassie protein assay reagent (Pierce). The MBP2 (43 kDa) produced from the pMAL-c2X with a stop codon inserted into the *XmnI* site was used as a control protein.

Enzyme-linked Immunosorbent Assay (ELISA)-based Binding Assay—A previously described ELISA-based binding assay was used to examine the binding affinity between the E2 protein and MBP-fused human LF fragment (48). Briefly, 96-well microtiter immunoplates (Maxisorp; Nunc) were coated overnight at 4 °C with the secreted form of the E2 protein (E2–681) (50 μl/well, 10 μg/ml) in HEPES-buffered saline (HBS) (10 mM HEPES, pH 7.0, 150 mM NaCl, 3.4 mM EDTA) (41). Both BSA and human TF (each: 50 μl/well, 10 μg/ml in HBS) were also used as negative controls. Rat monoclonal antibodies, MO-2 and MO-12, against E2 protein were used to determine the appropriate concentration of the E2 protein. 96-well microtiter plates were washed three times with HBS containing 0.05% Tween 20 and treated with 0.15% BSA in HBS (100 μl/well) to reduce the incidence of nonspecific binding. Following incubation on a shaking platform for 1 h at room temperature, MBP-fused human LF fragment (aa 600–632) or MBP2 (each: 5, 25, and 50 ng, 50 μl/well) was added. Following further incubation on a

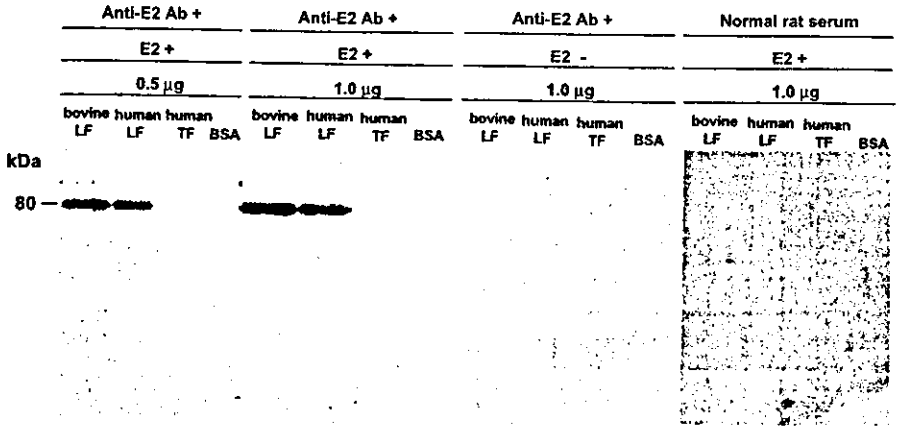

FIG. 1. **Direct interaction between LF and HCV E2 envelope protein.** Human and bovine LFs, and human TF and BSA (0.5 or 1 μg each; each sample was more than 90% pure) were resolved by 10% SDS-PAGE. Far-Western blot analysis using E2 protein expressed in Chinese hamster ovary cells (41) as a probe was performed as described under "Experimental Procedures." Rat monoclonal antibody MO-12 (42) against E2 protein (*Anti-E2 Ab*) was used for the detection of E2 protein bound to LF. Far-Western blot analyses in the absence of the E2 protein and using normal rat serum instead of rat monoclonal antibody MO-12 against E2 protein were also performed. The other rat monoclonal antibody, MO-2, which recognizes a different epitope from that recognized by MO-12, was also used for the detection, and the same results were obtained as those observed with MO-12 (data not shown).

shaking platform for 3 h at room temperature, the plates were washed as described above, and rabbit anti-MBP primary (New England Biolabs, Beverly, MA) and horseradish peroxidase-conjugated anti-rabbit IgG secondary (Amersham Biosciences) antibodies were used for the detection of binding between MBP-fused protein and the E2 protein. After the addition of the substrate, TMB One solution (Promega), A_{450} was measured using a Benchmark microplate reader (Bio-Rad).

Western Blot Analysis—SDS-PAGE and immunoblotting analysis were performed with polyvinylidene difluoride membranes as described previously (9). The rabbit polyclonal antibody (A0186; DAKO) against human LF and mouse polyclonal antibody (Pharmingen) against human CD81 were used for the detection of LF or CD81 by Western blot analysis. Rabbit anti-MBP antibody was also used for the detection of MBP by Western blot analysis. Immunocomplexes on the filters were detected by enhanced chemiluminescence assay (Renaissance; PerkinElmer Life Sciences).

Anti-HCV Activity of the MBP-fused LF Fragment—An assay for anti-HCV activity of the MBP-fused LF fragment was performed by a method described previously (36, 49) using LightCycler real-time PCR technology. Briefly, 2 μl (2 × 10^4 HCV) of HCV-positive serum 1B-2 (genotype 1b), described previously (23), and the MBP-fused human LF fragment (aa 600–632) (final concentration, 0.5–2.0 mg/ml) were preincubated in 100 μl of medium for 60 min at 4 °C and then the mixture of HCV and the LF fragment was added to the PH5CH8 cells (1.5 × 10^4 cells were cultured for 2 days at 37 °C before viral inoculation on a 96-well plate). The mixture was then incubated for 90 min at 37 °C. The cells were washed three times with 100 μl of PBS and cultured for 1 day at 32 °C. The cellular RNA was prepared using an ISOGEN extraction kit (Nippon Gene Co., Toyama, Japan), and 0.5 μg of RNA was used for the quantitative analysis of HCV RNA using LightCycler PCR (49). As the positive and negative controls for anti-HCV activity, human LF and MBP2, respectively, were used. All experiments in this assay system were performed in triplicate at least three times.

RESULTS

Direct Interaction between Human and Bovine LFs and HCV E2 Envelope Protein—We found previously (23, 24) that human and bovine LFs prevented HCV infection in human hepatocyte PH5CH8 cells (24) that were susceptible to HCV infection (23). Using LightCycler real-time PCR technology, we showed recently (49) that IC_{50} doses of human and bovine LFs were 5 and 1.5 μM, respectively, for HCV infection of hepatocyte cells. Our previous data (36) showed that the HCV-inhibiting activity of LF is because of the direct interaction between LF and HCV, suggesting that LF directly binds to HCV envelope proteins. This hypothesis is compatible with a previous report by another group (37) that HCV envelope proteins could bind human and bovine LFs, although their binding specificities have not been clarified. Therefore, we first examined the specificity of the direct interaction between LF and the E2 protein, which is thought to play a major role in HCV binding to target cells (38). Far-Western blot analysis was performed using the secreted form (aa 384–681) of E2 protein expressed in Chinese hamster ovary cells as a probe (41). As shown in Fig. 1, human and bovine LFs, which show ~80% aa homology, bound to E2 protein with similar intensity, whereas E2 protein binding activities of human TF showing ~60% aa homology to LF and BSA were not observed after a brief exposure. However, the long period of exposure clarified that human TF (see Fig. 4) and bovine TF (data not shown) did slightly bind to the E2 protein. This phenomenon suggests that the E2 protein binding activity of LF is overwhelmingly greater than that of TF. To exclude the possibility of cross-reactions between LF and anti-E2 antibody, we performed a Far-Western blot analysis in the absence of the E2 protein, as well as an analysis using normal rat serum instead of the anti-E2 antibody. As shown in Fig. 1, no significant bands were obtained in these control experiments, indicating that the bands obtained in this Far-Western blot analysis were derived from the interaction between LF and the E2 protein. Although the E2 proteins used by our group and Yi *et al.* (37) showed an ~14% amino acid difference because of the different HCV strains, bovine and human LFs were equally able to bind to these E2 proteins. These results suggest that LF binds specifically to the E2 protein, regardless of particular HCV strains.

Deglycosylation of LF Strengthens the Interaction between LF and E2 Protein—Both human and bovine LFs are glycoproteins possessing three and five *N*-linked oligosaccharide chains, respectively. These chains are composed of galactose, mannose, fucose, *N*-acetylglucosamine, and sialic acid (50). To examine whether these oligosaccharide chains reflect the E2 protein binding activity of LF, human and bovine LFs were deglycosylated with PNGaseF, which is preferred for the complete removal of the *N*-linked oligosaccharide chain. As shown in Fig. 2*A*, the molecular masses of human and bovine LFs decreased from 80 to 72 kDa, respectively, after treatment with PNGaseF, thereby indicating that the *N*-linked oligosaccharide chains of LF were removed. Using the deglycosylated and natural forms of human and bovine LFs, we compared the binding abilities of LFs to E2 protein. Far-Western blot analysis revealed that deglycosylation of human and bovine LFs resulted in intensified E2 protein binding activity (Fig. 2*B*). This result suggests that the interaction between LF and the E2 protein is

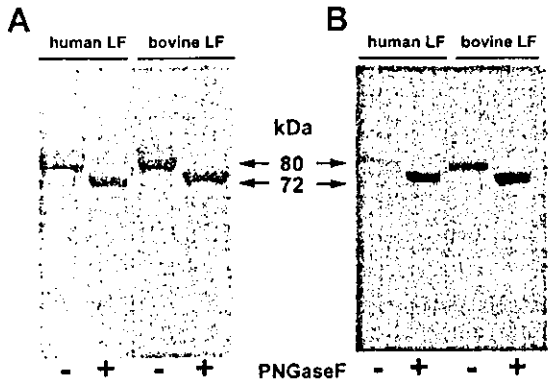

FIG. 2. **Deglycosylation of LF resulted in intensified binding to E2 protein.** *A*, human and bovine LFs deglycosylated with PNGaseF (each 0.5 μg) were resolved by 12% SDS-PAGE and were detected by Coomassie Brilliant Blue staining. *B*, effect of deglycosylation of LFs on the E2 protein binding ability. Far-Western blot analysis using E2 protein as a probe was carried out as indicated in Fig. 1.

not mediated through the *N*-linked oligosaccharides of LF and that at least one oligosaccharide interferes with the direct interaction between LF and the E2 protein. These results led us to undertake the preparation of various recombinant LF fragments using an *E. coli* expression system in which glycosylation does not occur.

Expression in E. coli and Purification of Human LF Fragments—We chose human LF for the preparation of the recombinant LF to investigate which region(s) of LF is (are) important for direct binding to the E2 protein, because the natural host of HCV is human, and a human source would be advantageous in the context of future medical applications. We obtained by RT-PCR a full-length LF cDNA using the total RNA (43) from human breast cancer tissue. Sequence analysis of the obtained LF cDNA clone confirmed that the deduced amino acid sequence was identical to the previously reported human LF (X52941) sequence (51).

To identify the region(s) of LF that bind to the E2 protein (Fig. 3*A*), we divided LF into eight fragments, namely, the N-lobe (N-terminal half without lactoferricin; aa 48–340), N-s1 (aa 48–123), N-s2 (aa 146–255), N-s3 (aa 256–340), the C-lobe (C-terminal half; aa 341–692), C-s1 (aa 341–486), C-s2 (aa 487–599), and C-s3 (aa 600–692), according to the well characterized three-dimensional domain of human LF (27). These LF fragments were successfully expressed as TRX-fused proteins in AD494 cells using the pET32a expression vector; it is already known that the solubility of an expressed protein increases in cells (52). Four LF fragments (N-s2, N-s3, C-s2, and C-s3) were successfully expressed in the soluble form in the cells, although the solubility of the remaining four LF fragments (N-lobe, N-s1, C-lobe, and C-s1) was still at a low level. All of the LF fragments expressed either as soluble or insoluble fractions were purified by affinity column chromatography using His-Bind resin, as indicated under "Experimental Procedures." As a result, eight TRX-fused LF fragments were purified as a single staining band with the expected molecular size after separation with SDS-PAGE (Fig. 3*B*).

A C-terminal Fragment of Human LF Predominantly Interacts with E2 Protein—Using the eight human LF fragments, we performed Far-Western blot analysis to examine which region(s) of LF possess the capacity to bind to E2 protein. The results revealed that two LF fragments, *i.e.* N-lobe (aa 48–340) and C-s3 (aa 600–692), specifically bound to the E2 protein, suggesting that at least two regions of human LF are involved in the direct interaction with the E2 protein (Fig. 3*C*). We noticed that the binding activity of C-s3 was similar to that of human LF, in contrast to the weak binding activity of the N-lobe. To avoid bias in the reactivity of the MO-12 rat monoclonal antibody, used for the detection of the E2 protein in the Far-Western blot analysis, the other rat monoclonal antibody, MO-2, which recognizes a different epitope from that recognized by MO-12, was also used. The obtained result was the same as that observed with MO-12 (data not shown). Because the C-s3 containing aa 600–692 of human LF was considered to be a major binding region, we focused on C-s3 to further characterize the E2 protein binding activity.

C-s3-relevant Fragments of Bovine and Horse LFs also Bind to E2 Protein—It is already known that the aa sequences of mammalian LFs show ~80% sequence homology with each other (53). We demonstrated that human and bovine LFs bind equally well to E2 protein (Fig. 1). Regarding C-s3, 74, 71, 58, and 53% aa sequence homology was demonstrated with the C-s3-relevant fragment of bovine and horse LFs and human and bovine TFs, respectively. To evaluate the E2 protein binding specificity of the C-s3, we examined the E2 protein binding activities of C-s3-relevant fragments of bovine and horse LF and human TF and compared their activities with that of C-s3. We first obtained bovine and horse LF cDNAs from bovine breast tissue and horse peripheral blood mononuclear cells, respectively, by RT-PCR. Human TF cDNA was also obtained by RT-PCR from the cultured PH5CH8 human hepatocytes. Using the obtained LF and TF cDNAs, three C-s3-relevant fragments of bovine and horse LFs and human TF were expressed as TRX-fused proteins in *E. coli* and were purified along with TRX-fused C-s3. Far-Western blot analysis showed that the C-s3-relevant fragments of bovine and horse LF also bound to the E2 protein, as well as C-s3, but the binding activity of the C-s3-relevant fragment of human TF was very weak (Fig. 4). This result suggests that the conserved amino acids among the three LF fragments were involved in the binding to the E2 protein. Comparison with the amino acid sequences of LFs and TFs of human, bovine, and horse revealed that LF-specific amino acids are mainly located in the first half of C-s3 (data not shown). This observation led us to carry out a homology search regarding the first half of the C-s3 fragments using the amino acid sequence databases. We were unable to obtain any interesting proteins showing high homology to this region, although a number of LF- and TF-related proteins were obtained in this survey. However, during the course of the survey, we did notice that the latter half (aa 146–201) of the LEL of the putative HCV receptor CD81 (19) showed partial homology with the first half (aa 600–647) of C-s3, although several gaps were necessary to make an alignment (Fig. 5*A*). This observation prompted us to compare the E2 protein binding activities of C-s3 and CD81 LEL.

E2 Protein Binding Activity of C-s3 Is Comparable with That of CD81 LEL—To compare the binding activities of C-s3 (93 aa) and CD81 LEL (89 aa), we obtained a cDNA encoding a CD81 LEL from PH5CH8 cells by RT-PCR. We confirmed that the nucleotide sequences of the obtained CD81 LEL cDNA were identical to that of previously reported human CD81 LEL (54). CD81 LEL was also expressed as a TRX-fused protein in *E. coli* using a pET-32a expression vector and was purified with the same efficiency as C-s3 (Fig. 5*B*). To confirm that the purified C-s3 and CD81 LEL are actually parts of human LF and CD81, respectively, we examined their immunological specificities by Western blot analysis. As shown in Fig. 5, *C* and *D*, anti-human LF and anti-human CD81 polyclonal antibodies specifically recognized TRX-fused C-s3 and CD81 LEL, indicating the successful preparation of recombinant C-s3 and CD81 LEL. Far-Western blot analysis revealed that both C-s3 and CD81 LEL bound to E2 protein, as shown in Fig. 5*E*. Interestingly, the binding activity of C-s3 was equal to or stronger than that of

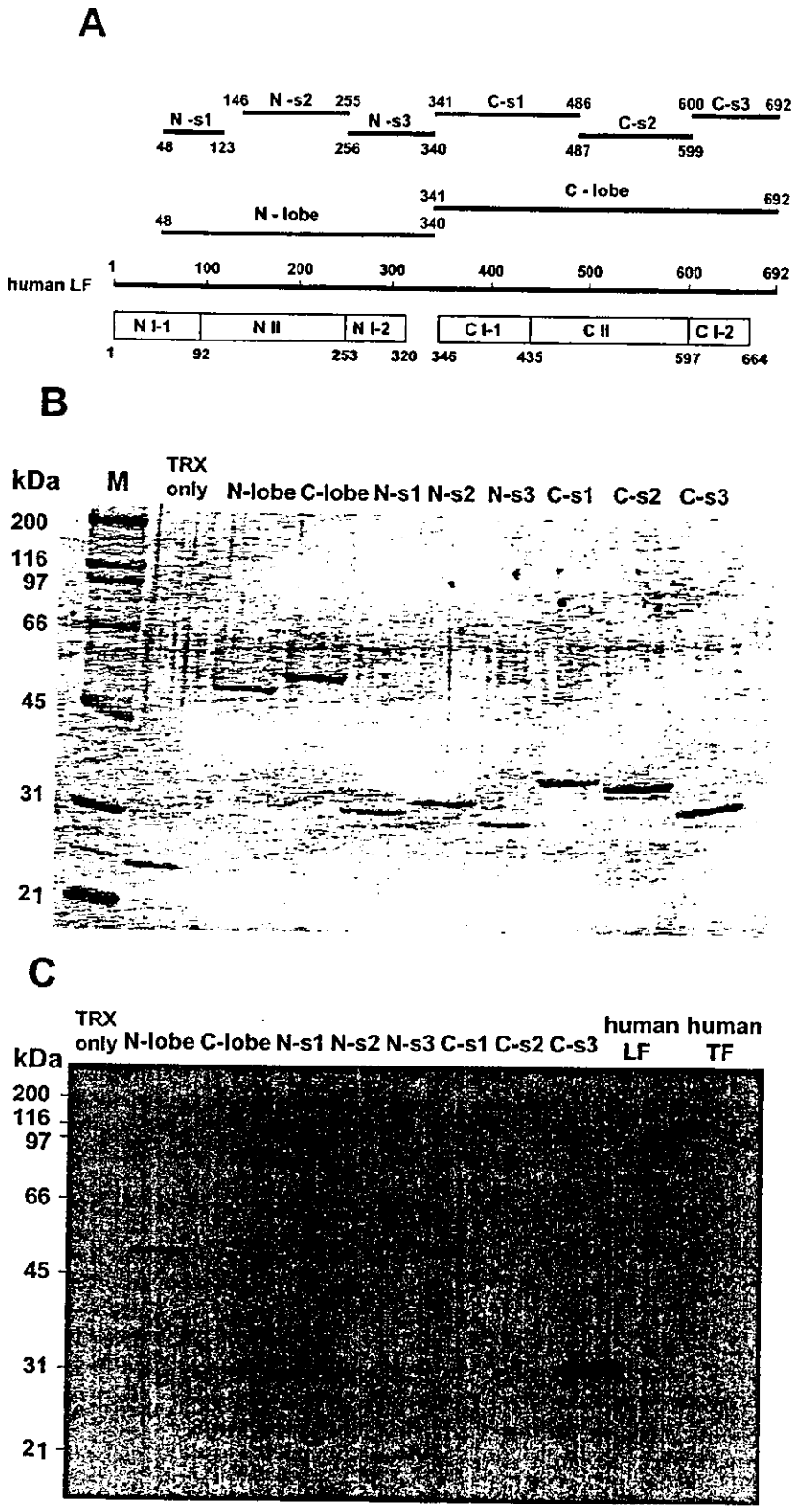

FIG. 3. **Expression of human LF fragments in *E. coli* and their E2 protein binding activities.** *A*, localization map of human LF fragments expressed in *E. coli*. *Numbers* indicate the aa positions of eliminated N-terminal signal sequences (19 amino acids) in LF. *NI-1*, *NII*, *NI-2*, *CI-1*, *CII*, and *CI-2* indicate the three-dimensional domain of human LF (27). *B*, purification of TRX-fused human LF fragments. Each 0.5 μg of LF fragments was resolved by 12% SDS-PAGE and was detected by Coomassie Brilliant Blue staining. *Lane M*, molecular marker of proteins. *C*, E2 protein binding activities of human LF fragments. The purified TRX-fused human LF fragments, human LF, and human TF were resolved by 12% SDS-PAGE and then Far-Western blot analysis using E2 protein as a probe was performed as indicated in Fig. 1. MO-12, a rat monoclonal antibody (42) against E2 protein, was used for the detection of E2 protein bound to LF or to LF fragments.

CD81 LEL. Because it appears that the E2 protein binding affinity of C-s3 is comparable with that of CD81 LEL, we proceeded to narrow down the potential binding domain to an area within the C-s3.

Identification of a Minimum E2 Protein Binding Domain within C-s3—To identify the E2 protein binding domain within C-s3, we first generated several truncated forms of C-s3, as shown in Fig. 6*A*. Each truncated form of C-s3 was expressed as a TRX-fused protein in *E. coli* and was purified as described under "Experimental Procedures." Far-Western blot analysis using these truncated C-s3 forms revealed that aa 600–652 retained the E2 protein binding activity (Fig. 6*B*). In addition, the binding activity of the C-s3 fragment (aa 610–692) was rather weak; the C-s3 fragment (aa 624–692) failed entirely at binding to the E2 protein (Fig. 6*B*, *lanes 4* and *5*). These results indicated that the N-terminal half of C-s3 suffices for binding

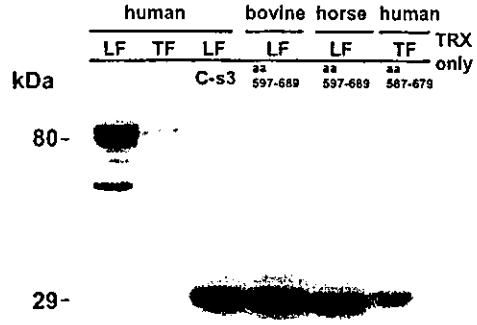

FIG. 4. **Binding to E2 protein of C-s3 and C-s3-relevant fragments of bovine and horse LFs and human TF.** Human LF and TF and purified TRX-fused C-s3 and C-s3-relevant fragments of bovine LF, horse LF, and human TF (0.5 μg each) were resolved by 12% SDS-PAGE. Far-Western blot analysis was carried out as indicated in Fig. 1.

to the E2 protein. Moreover, it was suggested that aa 600–624 of human LF, overlapping with the CD81 homology region (aa 615–644), is necessary for binding to the E2 protein. To further narrow down the binding domain from the C-s3 fragment (aa 600–652), we systematically created a series of truncated forms based on the C-s3 fragment (aa 600–652), as shown in Fig. 7*A*. These truncated forms were then expressed as TRX-fused proteins and were purified along with the other TRX-fused proteins. In this series of experiments, we created an additional TRX-fused LF fragment consisting of aa 590–652 to clarify whether aa 600 is an N-terminal limit for E2 protein binding activity. As shown in Fig. 7*B*, the results showed that the E2 protein binding activity of human LF (aa 590–652) was almost equal to that of the C-s3 fragment (aa 600–652), suggesting that the region of aa 590–599 did not contribute to binding to the E2 protein. Although the C-s3 fragment (aa 600–652) possessed such binding activity, the C-s3 fragment (aa 605–652) had almost no ability to bind to the E2 protein. Regarding the carboxyl-truncated forms of the C-s3 fragment (aa 600–652), it appeared that the C-s3 fragment (aa 600–627) did not bind to the E2 protein and that the C-s3 fragment (aa 600–632) bound equally well to the E2 protein as the C-s3 fragment (aa 600–652) (Fig. 7*B*). Therefore, aa 600–632 of human LF appeared to be the minimum region required for E2 protein binding activity. These results suggest that both aa 600–604 and aa 628–632 contain critical amino acid residues required for binding to the E2 protein.

MBP-fused C-s3 Fragment (aa 600–632) also Binds to the E2 Protein—To exclude the possibility that the E2 protein binding activity of the C-s3 fragment (aa 600–632) was an experimental artifact in the presence of TRX, we prepared the MBP-fused C-s3 fragment (aa 600–632) using the *E. coli* expression system and examined its ability to bind to the E2 protein. We confirmed the purity of the MBP-fused C-s3 fragment (aa 600–632) with Coomassie Brilliant Blue staining (Fig. 8*A*), and we demonstrated its quality with Western blot analysis using anti-human LF antibody (Fig. 8*B*) and anti-MBP antibody (Fig. 8*C*). As shown in Fig. 8*D*, it became apparent that the MBP-fused C-s3 fragment (aa 600–632) and the TRX-fused C-s3 fragment (aa 600–632) bound equally well to the E2 protein, whereas MBP2 (control protein without LF) or TRX (control protein without LF) alone did not bind to the E2 protein. To verify the E2 protein binding activity of the C-s3 fragment (aa 600–632), we performed an ELISA-based binding assay using the MBP-fused C-s3 fragment (aa 600–632) and the E2 protein. As shown in Fig. 9*A*, the MBP-fused C-s3 fragment (aa 600–632) bound to the E2 protein in a dose-dependent manner, whereas the binding activity of MBP2 (control protein without LF) alone was at a significantly low level. Furthermore, an ELISA-based binding assay was used to confirm the E2 protein binding specificity of the MBP-fused C-s3 fragment (aa 600–632). As shown in Fig. 9*B*, the MBP-fused C-s3 fragment (aa 600–632) strongly bound to the E2 protein, whereas the MBP-fused C-s3 fragment (aa 600–632) showed low binding affinity against human TF and BSA. The binding levels of MBP2 to human TF and BSA, as well as that to the E2 protein, were also fairly low. In addition, using this ELISA assay, we confirmed that human LF also bound to the E2 protein in a dose-dependent manner (data not shown). Taken together, these results indicate that the C-s3 fragment (aa 600–632) is directly involved in binding to the E2 protein. We observed that bovine LF (aa 597–629) corresponding to the C-s3 fragment (aa 600–632) and the C-s3 fragment (aa 600–632) were able to bind equally well to the E2 protein (data not shown). It is also noteworthy that the region of the C-s3 fragment (aa 600–632) was located on a surface portion of the C-lobe domain in the three-dimensional structure of human LF (27); the region of aa 606–622 has an α-helix structure, and both terminal ends (five aa each) of the C-s3 fragment (aa 600–632), thought to be important for the E2 protein binding activity, are highly conserved between human and bovine LFs (Fig. 10).

The MBP-fused C-s3 Fragment (aa 600–632) prevents HCV infection in the cells—To evaluate whether the C-s3 fragment (aa 600–632), identified as the minimum binding site to the E2 protein, can prevent HCV infection, we initially examined the anti-HCV activity of the TRX-fused C-s3 fragment (aa 600–632) in our HCV infection system using PH5CH8 cells. Although we carried out a quantitative analysis of HCV RNA using LightCycler PCR, we did not successfully demonstrate the anti-HCV activity of the TRX-fused C-s3 fragment (aa 600–632), because TRX itself showed some cell toxicity in our viral infection system. As regards this cell toxicity, we considered that it might have been because of detergent remaining in the sample after the preparation of the TRX-fused proteins. However, no detergents were used during the process of the purification of MBP-fused protein; we next examined the anti-HCV activity of the MBP-fused C-s3 fragment (aa 600–632) using the same assay system described above. As shown in Fig. 11, the obtained results revealed that the MBP-fused C-s3 fragment (aa 600–632) was able to inhibit HCV infection in PH5CH8 cells in a dose-dependent manner, whereas MBP2 was not able to inhibit HCV infection of the cells. In addition, the IC_{50} dose of the MBP-fused C-s3 fragment (aa 600–632) was estimated to be ~20 μM (1.0 mg/ml), although the IC_{50} dose of human LF was 5 μM (0.4 mg/ml). These results suggest that E2 protein binding activity of the MBP-fused C-s3 fragment (aa 600–632) contributes to the inhibition of HCV infection of these cells. Furthermore, the findings suggest that aa 600–632 of human LF possess anti-HCV activity, although this type of anti-HCV activity was somewhat weaker than that of human LF.

Cys on aa 628 Is Critical for the Binding to E2 Proteins—Because both aa 600–604 and aa 628–632 of human LF were estimated to be important for binding to the E2 protein, and five (aa 602, 604, 629, 630, and 631) of these 10 positions show aa differences between human LF and TF, we considered that the specificity of amino acids also provides E2 protein binding activity. To gain further insight into the roles of these aa sequences, a series of 14 point-substitution mutations (aa 600–605 and 625–632) of the C-s3 fragment (aa 600–632) were constructed by site-directed mutagenesis to Ala. Far-Western blot analysis using these Ala mutants revealed that the Cys of

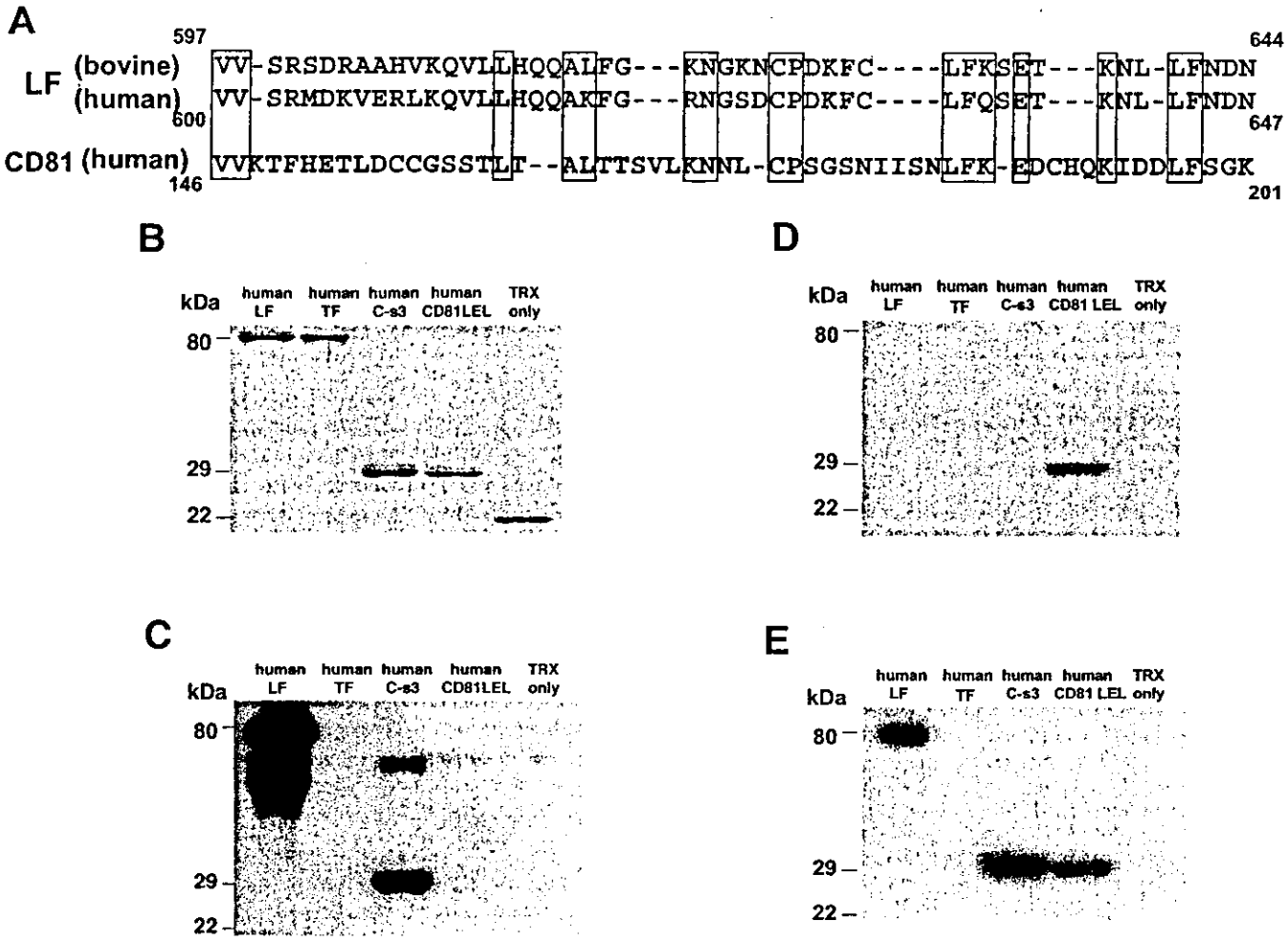

FIG. 5. **Comparison of E2 protein binding abilities of C-s3 and CD81 LEL.** *A*, amino acid sequence alignment of the first half of C-s3 and C-s3-relevant regions of bovine LF and the latter half of CD81 LEL. The same amino acids are *boxed* in each case. *Hyphens* indicate gaps. *B*, purification of TRX-fused human CD81 LEL. Human LF, human TF, TRX-fused C-s3, and TRX-fused CD81 LEL (0.5 μg each) were resolved by 12% SDS-PAGE and were detected by Coomassie Brilliant Blue staining. *C*, immunological specificity of TRX-fused C-s3. Western blot analysis using rabbit anti-human LF polyclonal antibody was carried out using the same proteins as those shown in *B*. *D*, immunological specificity of TRX-fused CD81 LEL to E2 protein. Western blot analysis using anti-human CD81 polyclonal antibody was carried out using the same proteins as those shown in *B*. *E*, E2 protein binding activities of C-s3 and CD81 LEL. Far-Western blot analysis using the E2 protein as a probe was carried out using the same proteins as those shown in *B*.

aa 628 is quite important for binding to the E2 protein, because a Cys to Ala substitution on aa 628 completely abolished E2 protein binding activity (Fig. 12). In addition, four Ala mutants (aa 626, 627, 629, and 630) increased binding activity, suggesting that the binding affinity of the C-s3 fragment (aa 600–632) to the E2 protein was not optimal.

DISCUSSION

Based on the our studies (24, 36) and those of other groups (37), we undertook observations regarding the direct interactions between LF and HCV envelope proteins. In this study, we demonstrated the binding specificity between LF and the E2 protein and identified 33 aa residues from human LF that are primarily responsible for E2 protein binding activity and inhibiting HCV infection of target cells.

We observed that the deglycosylation of human and bovine LFs enhanced E2 protein binding activity. This observation suggests that a certain *N*-linked oligosaccharide chain interferes with the interaction between LF and the E2 protein. Comparison with the putative *N*-linked glycosylation sites between human LF (3 sites; aa 138, 479, and 624) and bovine LF (5 sites; aa 233, 281, 368, 476, and 545) revealed that only one glycosylation site (aa 479 for human LF, aa 476 for bovine LF) is conserved in both LFs. Therefore, it is likely that this conserved glycosylation site, which is located in C-s1, weakens the E2 protein binding activity of human or bovine LF. This may also explain why we were able to detect the strong binding affinity of C-s3 for the E2 protein. However, the reason why the C-lobe did not bind to the E2 protein remains unclear. One possibility would be that the refolding of the TRX-fused C-lobe was not successful. Our results indicate that at least two regions of human LF (the N-lobe and C-s3) are involved in the interaction with the E2 protein, although we could not identify the binding region in the N-lobe. Although N-s3 shows ~35% aa homology to C-s3, N-s3 is unable to bind to the E2 protein. In addition, 12 aa are shared in common between the N-s3 fragment (aa 256–287) and the C-s3 fragment (aa 600–632) identified as a critical domain for binding to E2 protein. However, a Cys residue at aa 628 appeared to be essential for binding to the E2 protein; it is of note that this Cys is not present in the corresponding position of N-s3. Therefore, some boundary region between N-s1 and N-s2, or between N-s2 and N-s3, may possess the binding ability to the E2 protein. Interestingly, the C-s3 fragment (aa 600–632) was located close to the boundary region between N-s2 and N-s3 in the three-dimensional structure of human LF (27), suggesting that the E2 protein is able to bind to both

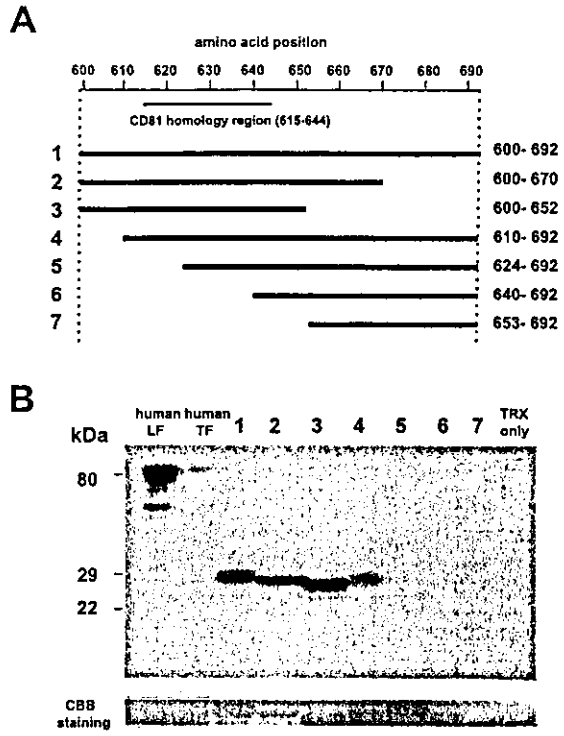

FIG. 6. **Deletion analysis of C-s3 possessing E2 protein binding activity.** *A*, localization map of the C-s3 variants truncated from N-terminal or C-terminal portions of C-s3. These LF fragments were expressed as TRX-fused proteins in *E. coli* and were purified for the Far-Western blot analysis. *Numbers* indicate the aa positions of human LF. *B*, E2 protein binding activities of C-s3 truncated variants. Far-Western blot analysis using the E2 protein as a probe was carried out as indicated in Fig. 1. To indicate that equal amounts of TRX-fused C-s3 variants were resolved by 12% SDS-PAGE, these LF fragments were stained with Coomassie Brilliant Blue (*CBB*; *lower panel*).

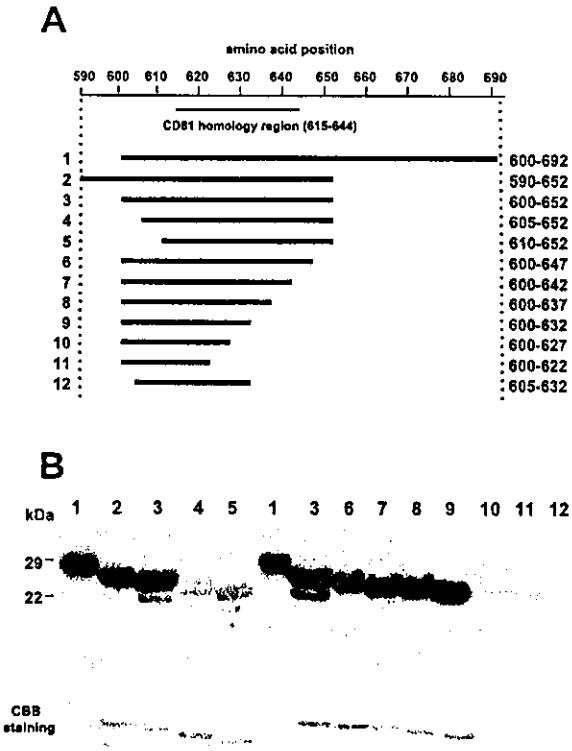

FIG. 7. **Identification of a minimum E2 protein binding domain in C-s3.** *A*, localization maps of the C-s3-truncated variants and a human LF (aa 590–652) were examined regarding E2 protein binding activity. These LF fragments were expressed as TRX-fused proteins in *E. coli* and purified for Far-Western blot analysis. *Numbers* indicate the aa positions of human LF. *B*, E2 protein binding activities of C-s3-truncated variants and a human LF (aa 590–652). Far-Western blot analysis using the E2 protein as a probe was carried out as indicated in Fig. 1. To indicate that equal amounts of TRX-fused C-s3 variants were resolved by 12% SDS-PAGE, these LF fragments were stained by Coomassie Brilliant Blue (*CBB*; *lower panel*).

sites of human LF. To clarify this assumption, further analysis will be needed.

We demonstrated that C-s3-relevant fragments (93 aa) of bovine and horse LFs bound as well to the E2 protein as did C-s3. The C-s3-relevant fragments of bovine and horse LFs show 74 and 71% aa sequence homology to C-s3 of human LF, respectively. These values are significantly higher than those (58 and 53%, respectively) of C-s3-relevant fragments of human and bovine TFs, which possess little binding activity to the E2 protein. The identified critical domain (aa 600–632) of human LF also shows 70% aa sequence homology to bovine LF (aa 597–629), whereas it shows only 42% aa sequence homology to the relevant regions of human or bovine TF (Fig. 10). These data suggest that the binding activity to E2 protein is restricted to the LF family.

During the process of characterization of a C-s3 LF fragment possessing E2 protein binding activity, we noticed that C-s3 showed partial aa homology with LEL of CD81, which can also bind to E2 protein and is considered as a candidate HCV receptor (19). The E2 protein binding activity of CD81 LEL has been well characterized *in vitro* (55) and *in vivo* (56), and the binding specificity of CD81 to E2 protein has been clarified (57). However, it has been reported that CD81 is not directly involved in the cell fusion caused by HCV (58). Because it has been shown that TRX-fused C-s3 (93 aa) has a comparable E2 protein binding ability with that of TRX-fused CD81 LEL (89 aa), C-s3 may interfere with the binding of the E2 protein to CD81. This may be one of the reasons why LF prevents HCV infection in target cells. However, one major contradiction remains. Regarding the interaction between human CD81 LEL and the E2 protein, it has been shown that aa 186 (Phe) of the CD81 is the critical residue for binding to the E2 protein (57). This Phe residue is conserved between human CD81 and LF (aa 635) (Fig. 5*A*). However, in this study, it appeared that the Phe at aa 635 of human and bovine LFs was unimportant for binding to the E2 protein, because the C-s3 fragment (aa 600–632) possessing the E2 protein binding activity does not contain this Phe residue. In addition, it has been reported that the four Cys of CD81 LEL form two disulfide bridges, the integrity of which would be necessary for CD81-E2 interaction (54). However, such a phenomenon was not observed in C-s3 containing five Cys residues, because the C-s3 fragment (aa 600–632) identified as the E2 protein binding domain contains only one Cys. Therefore, these data suggest that the E2 protein region targeted by human LF and CD81 may differ. Preliminarily, our experiment with Far-Western blot analysis showed that the C-s3 fragment (aa 600–632) preferentially bound to aa 411–500 of the E2 protein, which is one of two regions (aa 384–500 and 600–661) identified previously (37) as regions binding to human LF; however, the C-s3 fragment (aa 600–632) did not bind to aa 501–599 of E2 protein (data not shown). Because it has been indicated that both aa 480–493 and aa 544–551 of the E2 protein are involved in the binding to CD81 (56), human LF and CD81 may recognize rather different sites on the E2 protein. Further analysis will be necessary to clarify this point.

Because aa 600–632 of human LF possesses only one Cys at aa 628, it is unlikely that a disulfide bond is required for the E2 protein binding activity of the C-s3 fragment (aa

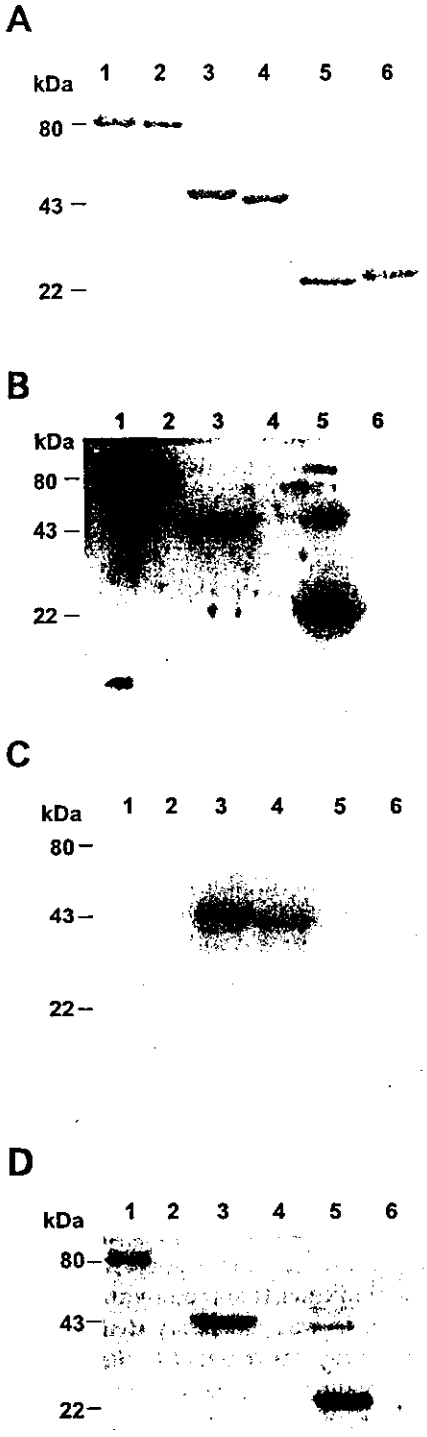

FIG. 8. **E2 protein binding specificity of the C-s3 fragment (aa 600–632).** The E2 protein binding activity of the MBP-fused C-s3 fragment (aa 600–632) was examined by Far-Western blot analysis as indicated in Fig. 1. *Lane 1*, human LF; *lane 2*, human TF; *lane 3*, MBP-fused C-s3 fragment (aa 600–632); *lane 4*, MBP2 without LF; *lane 5*, TRX-fused C-s3 fragment (aa 600–632); *lane 6*, TRX without LF. *A*, Coomassie Brilliant Blue staining after 12% SDS-PAGE. *B*, Western blot analysis using rabbit anti-human LF polyclonal antibody. *C*, Western blot analysis using rabbit anti-MBP polyclonal antibody. *D*, Far-Western blot analysis using the E2 protein as a probe.

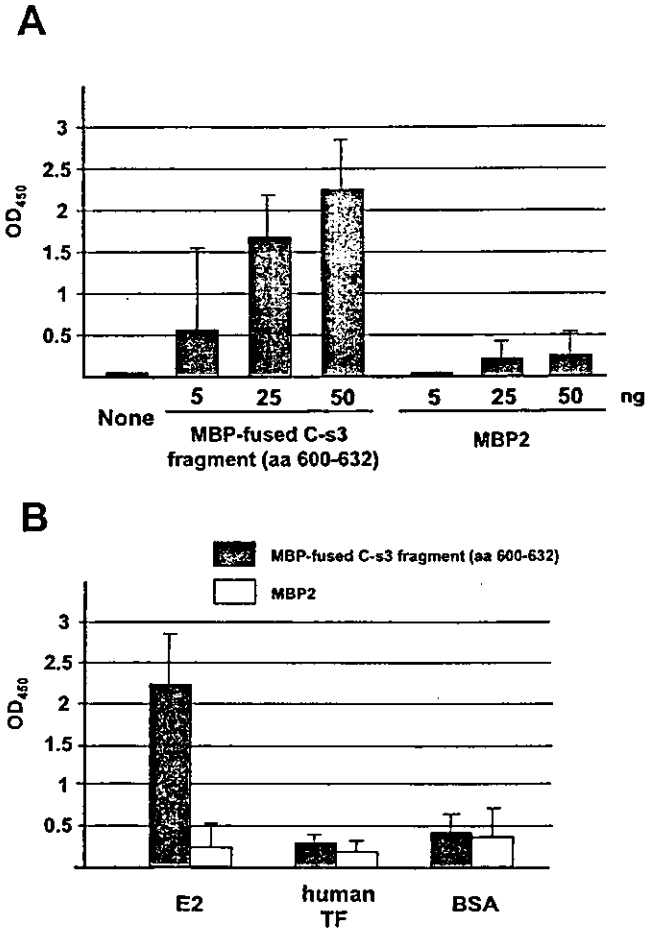

FIG. 9. **ELISA-based E2 protein binding activity of the C-s3 fragment (aa 600–632).** *A*, the MBP-fused C-s3 fragment (aa 600–632) bound to the E2 protein in a dose-dependent manner. An ELISA-based binding assay was performed to examine the E2 protein binding activity of the MBP-fused C-s3 fragment (aa 600–632), as described under "Experimental Procedures." MBP2 was used as a control protein without LF. 5, 25, and 50 ng of the MBP-fused C-s3 fragment (aa 600–632) or MBP2 were used for binding to the E2 protein. *B*, binding specificity of the MBP-fused C-s3 fragment (aa 600–632). To examine the E2 protein binding specificity of the MBP-fused C-s3 fragment (aa 600–632), human TF and BSA were also coated to immunoplates and were used as negative controls in the ELISA-based binding assay. MBP2 was used as a control protein without LF. 50 ng of the MBP-fused C-s3 fragment (aa 600–632) or MBP2 were used for binding to the E2 protein, human TF, or BSA.

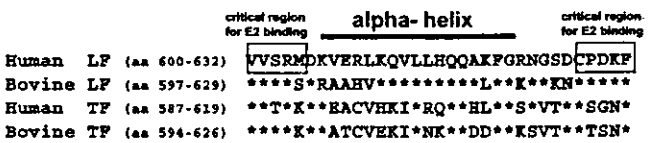

FIG. 10. **Amino acid sequence alignment of C-s3 and C-s3-relevant fragments of bovine LF, human TF, and bovine TF.** *Capital letters* indicate amino acids that differed from those in the sequences of aa 600–632 of human LF. The identical amino acids are indicated with *asterisks*. The α-helix structure (aa 606–622) identified in human LF (22) is depicted by a *thick bar*. Both the N-terminal five aa and C-terminal five aa, which are considered to be critical for E2 protein binding, are shown in *boxes*.

600–632). However, we cannot exclude the possibility that Cys at aa 628 paired with other Cys residues in TRX during the refolding process of the Far-Western blot analysis; this could have provided E2 protein binding activity. To exclude this possibility, we constructed the MBP-fused C-s3 fragment (aa 600–632), because Cys was not present in the MBP portion including the linker region. Although the MBP-fused C-s3 fragment (aa 600–632) possesses only one Cys, this fusion protein showed similar E2 protein binding activity with that of the TRX-fused C-s3 fragment (aa 600–632). Therefore, the present results suggest that a disulfide bond is not required for binding to the E2 protein, in contrast to the

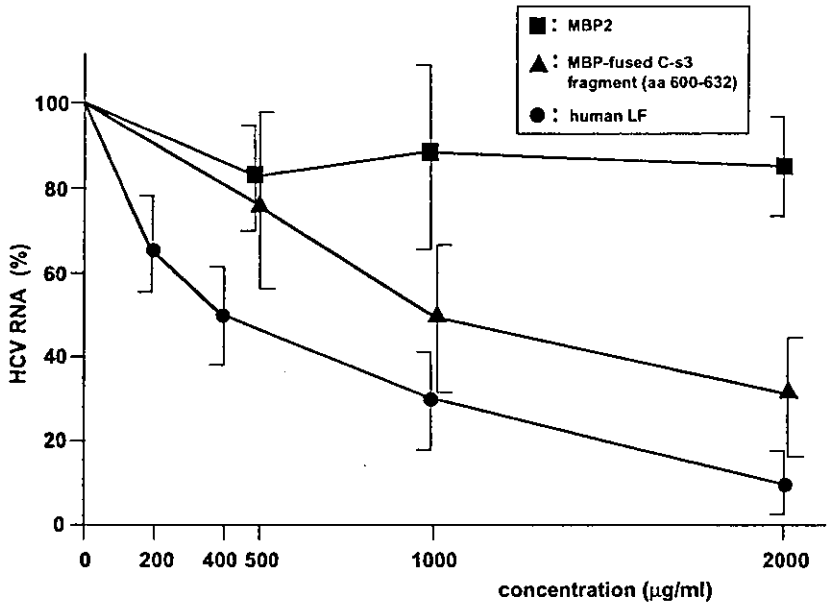

FIG. 11. **Anti-HCV activity of the MBP-fused C-s3 fragment (aa 600–632) in PH5CH8 cells.** PH5CH8 cells and inoculum 1B-2 were used for the HCV-inhibiting assay, as described under "Experimental Procedures." The *number* in the *axis* of the *ordinate* indicates the percent of the amount of HCV RNA determined by quantitative RT-PCR using LightCycler PCR (49). Approximately 2,000 copies of HCV RNA per μg of cellular RNA was reproducibly obtained using this HCV infection system (36, 49). In addition to the MBP-fused C-s3 fragment (aa 600–632), human LF and MBP2 were also used for the assay as control materials.

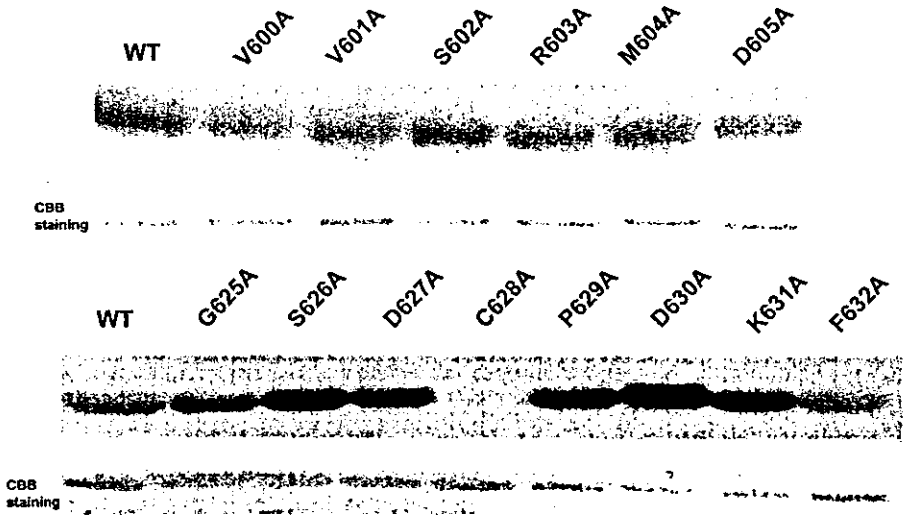

FIG. 12. **Site-directed mutagenesis of the TRX-fused C-s3 fragment (aa 600–632).** Site-directed mutagenesis to Ala was carried out in aa 600–605 and 625–632, respectively. *Lane WT*, TRX-fused C-s3 fragment (aa 600–632). Far-Western blot analysis was performed using the E2 protein as a probe (*upper panel*), as indicated in Fig. 1. The purified TRX-fused proteins were stained with Coomassie Brilliant Blue (*CBB*) after 12% SDS-PAGE to confirm their purities (*lower panel*).

case involving CD81 LEL (55). However, it is of note that site-directed mutagenesis to Ala in both terminal regions of the C-s3 fragment (aa 600–632) revealed that Cys at aa 628 is the most critical residue for binding to the E2 protein. To clarify whether only the Cys residue at this position is necessary for binding to the E2 protein, further experiments (*e.g.* substitution of amino acids other than Ala) will be needed.

Because it is well known that E1 and E2 proteins form a non-covalently linked heterodimer, which probably represents the surface of infectious virus particles (59), it is important to clarify whether the C-s3 fragment (aa 600–632) identified in this study binds to the heterodimer of E1 and E2 proteins. To date, aa 441–500 of E2 protein has been identified as the E1 protein heterodimeric binding region (60). Although our preliminary results estimated that the C-s3 fragment (aa 600–632) binds to aa 411–500 of the E2 protein, the E2 protein binding activity of the C-s3 fragment (aa 600–632) may not be affected by heteromeric complex formation between E1 and E2 proteins, because LF prevents HCV infection by direct interaction between LF and HCV (36).

We demonstrated the anti-HCV activity of the MBP-fused C-s3 fragment (aa 600–632) in our HCV infection system using PH5CH8 cells (36, 49). Although this result suggests that the E2 protein binding activity contributes to the prevention of HCV infection, our results revealed that the anti-HCV activity of the MBP-fused C-s3 fragment (aa 600–632) was severalfold weaker than that of human LF. However, site-directed mutagenesis to an Ala residue within aa 600–605 and aa 625–632 of human LF revealed that several positions strengthened the E2 protein binding activity. This result suggests that some peptides possess stronger binding activity than that of the C-s3 fragment (aa 600–632) and that these peptides could be obtained by screening peptide libraries, *e.g.* phage libraries. The antiviral activities of such peptides will be evaluated using our cell culture assay system (36, 49). Furthermore, such peptides may be useful for the removal of circulating HCV. In any case, the present study broadens the possibilities for developing anti-HCV peptides in the future.

Acknowledgments—We are grateful to Dr. H. Kariwa (Hokkaido University) for providing normal bovine breast tissue and normal horse peripheral blood mononuclear cells. We thank Dr. K. Shimotohno (Kyoto University), Dr. K. Sugiyama (National Cancer Center Research Institute, Tokyo, Japan), and Dr. T. Tanaka (National Institute of Neurology and Psychiatry) for helpful suggestions and for discussions about the study. We thank A. Morishita for helpful experimental assistance.

REFERENCES

1. Choo, Q. L., Kuo, G., Weiner, A. J., Overby, L. R., Bradley, D. W., and Houghton, M. (1989) *Science* **244,** 359–362
2. Kuo, G., Choo, Q. L., Alter, H. J., Gitnick, G. L., Redeker, A. G., Purcell, R. H., Miyamura, T., Dienstag, J. L., Alter, M. J., Stevens, C. E., Tegtmeier, G. E., Bonino, F., Colombo, W. S., Lee, W. S., Kuo, C., Berger, K., Shuster, J. R., Overby, L. R., Bradley, D. W., and Houghton, M. (1989) *Science* **244,** 362–364
3. Ohkoshi, S., Kojima, H., Tawaraya, H., Miyajima, T., Kamimura, T., Asakura, H., Satoh, A., Hirose, S., Hijikata, M., Kato, N., and Shimotohno, K. (1990) *Jpn. J. Cancer Res.* **81,** 550–553
4. Saito, I., Miyamura, T., Ohbayashi, A., Harada, H., Katayama, T., Kikuchi, Y. Watanabe, S., Koi, S., Onji, M., Ohta, Y., Choo, Q. L., Houghton, M., and Kuo, G. (1990) *Proc. Natl. Acad. Sci. U. S. A.* **87,** 6547–6549
5. Kato, N., Hijikata, M., Ootsuyama, Y., Nakagawa, M., Ohkoshi, S., Sugimura, T., and Shimotohno, K. (1990) *Proc. Natl. Acad. Sci. U. S. A.* **87,** 9524–9528
6. Miller, R. H., and Purcell, R. H. (1990) *Proc. Natl. Acad. Sci. U. S. A.* **87,** 2057–2061
7. Tanaka, T., Kato, N., Cho, M. J., and Shimotohno, K. (1995) *Biochem. Biophys. Res. Commun.* **215,** 744–749
8. Hijikata, M., Kato, N., Ootsuyama, Y., Nakagawa, M., and Shimotohno, K. (1991) *Proc. Natl. Acad. Sci. U. S. A.* **88,** 5547–5551
9. Hijikata, M., Mizushima, H., Tanji, Y., Komoda, Y., Hirowatari, Y., Akagi, T., Kato, N., Kimura, K., and Shimotohno, K. (1993) *Proc. Natl. Acad. Sci. U. S. A.* **90,** 10773–10777
10. Grakoui, A., Wychowski, C., Lin, C., Feinstone, S. M., and Rice, C. M. (1993) *J. Virol.* **67,** 1385–1395
11. Lin, C., Lindenbach, B. D., Pragai, B. M., McCourt, D. W., and Rice, C. M. (1994) *J. Virol.* **68,** 5063–5073
12. Mizushima, H., Hijikata, M., Tanji, Y., Kimura, K., and Shimotohno, K. (1994) *J. Virol.* **68,** 2731–2734
13. Bukh, J., Miller, R. H., and Purcell, R. H. (1995) *Semin. Liver Dis.* **15,** 41–63
14. Simmonds, P. (1995) *Hepatology* **21,** 570–583
15. Purcell, R. (1997) *Hepatology* **26,** Suppl. 1, 11s–14s
16. Kato, N. (2000) *Microb. Comp. Genomics* **5,** 129–151
17. Shiratori, Y., Kato, N., Yokosuka, O., Imazeki, F., Hashimoto, E., Hayashi, N., Nakamura, A., Asada, M., Kuroda, H., Tanaka, N., Arakawa, Y., and Omata, M. (1997) *Gastroenterology* **113,** 558–566
18. McHutchison, J. G., Gordon, S. C., Schiff, E. R., Shiffman, M. L., Lee, W. M., Rustgi, V. K., Goodman, Z. D., Ling, M. H., Cort, S., and Albrecht, J. K. (1998) *N. Engl. J. Med.* **339,** 1485–1492
19. Pileri, P., Uematsu, Y., Campagnoli, S., Galli, G., Falugi, F., Petracca, R., Weiner, A. J., Houghton, M., Rosa, D., Grandi, G., and Abrignani, S. (1998) *Sience* **282,** 938–941
20. Scarselli, E., Ansuini, H., Cerino, R., Roccasecca, R. M., Acali, S., Filocamo, G., Traboni, C., Nicosia, A., Cortese, R., and Vitelli, A. (2002) *EMBO J.* **21,** 5017–5025
21. Agnello, V., Abel, G., Elfahal, M., Knight, G. B., and Zhang, Q. X. (1999) *Proc. Natl. Acad. Sci. U. S. A.* **96,** 12766–12771
22. Kato, N., and Shimotohno, K. (2000) *Curr. Top. Microbiol. Immunol.* **242,** 261–278
23. Ikeda, M., Sugiyama, K., Mizutani, T., Tanaka, T., Tanaka, K., Sekihara, H., Shimotohno, K., and Kato, N. (1998) *Virus Res.* **56,** 157–167
24. Ikeda, M., Sugiyama, K., Tanaka, T., Tanaka, K., Sekihara, H., Shimotohno, K., and Kato, N. (1998) *Biochem. Biophys. Res. Commun.* **245,** 549–553
25. Matsuura, Y., Tani, H., Suzuki, K., Kimura-Someya, T., Suzuki, R., Aizaki, H., Ishii, K., Moriishi, K., Robison, C. S., Whitt, M. A., and Miyamura, T. (2001) *Virology* **286,** 263–275
26. Levay, P. F., and Viljoen, M. (1995) *Haematologica* **80,** 252–267
27. Anderson, B. F., Baker, H. M., Norris, G. E., Rice, D. W., and Baker, E. N. (1989) *J. Mol. Biol.* **209,** 711–734
28. Moore, S. A., Anderson, B. F., Groom, C. R., Haridas, M., and Baker, E. N. (1997) *J. Mol. Biol.* **274,** 222–236
29. Aisen, P., and Leibman, A. (1972) *Biochim. Biophys. Acta* **257,** 314–323
30. Bellamy, W., Takase, M., Yamauchi, K., Wakabayashi, H., Kawase, K., and Tomita, M. (1992) *Biochim. Biophys. Acta.* **1121,** 130–136
31. Sanchez, L., Aranda, P., Perez, M. D., and Calvo, M. (1988) *Biol. Chem. Hoppe-Seyler* **369,** 1005–1008
32. Nagasawa, T., Kiyosawa, I., and Kuwahara, K. (1972) *J. Dairy Sci.* **55,** 1651–1659
33. Sekine, K., Watanabe, E., Nakamura, J., Takasuka, N., Kim, D. J., Asamoto, M., Krutovskikh, V., Baba-Toriyama, H., Ota, T., Moore, M. A., Masuda, M., Sugimoto, H., Nishino, H., Kakizoe, T., and Tsuda, H. (1997) *Jpn. J. Cancer Res.* **88,** 523–526
34. Tanaka, K., Ikeda, M., Nozaki, A., Kato, N., Tsuda, H., Saito, S., and Sekihara, H. (1999) *Jpn. J. Cancer Res.* **90,** 367–371
35. Iwasa, M., Kaito, M., Ikoma, J., Takeo, M., Imoto, I., Adachi, Y., Yamauchi, K., Koizumi, R., and Teraguchi, S. (2002) *Am. J. Gastroenterol.* **97,** 766–767
36. Ikeda, M., Nozaki, A., Sugiyama, K., Tanaka, T., Naganuma, A., Tanaka, K., Sekihara, H., Shimotohno, K., Saito, M., and Kato, N. (2000) *Virus Res.* **66,** 51–63
37. Yi, M., Kaneko, S., Yu, D. Y., and Murakami, S. (1997) *J. Virol.* **71,** 5997–6002
38. Rosa, D., Campagnoli, S., Moretto, C., Guenzi, E., Cousens, L., Chin, M., Dong, C., Weiner, A. J., Lau, J. Y. N., Choo, Q. L., Chien, D., Pileri, P., Houghton, M., and Abrignani, S. (1996) *Proc. Natl. Acad. Sci. U. S. A.* **93,** 1759–1763
39. Farci, P., Shimoda, A., Wong, D., Cabezon, T., De Gioannis, D., Strazzera, A., Shimizu, Y., Shapiro, M., Alter, H. J., and Purcell, R. H. (1996) *Proc. Natl. Acad. Sci. U. S. A.* **93,** 15394–15399
40. Ishii, K., Rosa, D., Watanabe, Y., Katayama, T., Harada, H., Wyatt, C., Kiyosawa, K., Aizaki, H., Matsuura, Y., Houghton, M., Abrignani, S., and Miyamura, T. (1998) *Hepatology* **28,** 1117–1120
41. Inudoh, M., Nyunoya, H., Tanaka, T., Hijikata, M., Kato, N., and Shimotohno, K. (1996) *Vaccine* **14,** 1590–1596
42. Inudoh, M., Kato, N., and Tanaka, Y. (1998) *Microbiol. Immunol.* **42,** 875–877
43. Kato, N., Pfeifer-Ohlsson, S., Kato, M., Larsson, E., Rydnert, J., Ohlsson, R., and Cohen, M. (1987) *J. Virol.* **61,** 2182–2191
44. Kato, N., Hijikata, M., Ootsuyama, Y., Nakagawa, M., Ohkoshi, S., and Shimotohno, K. (1990) *Mol. Biol. Med.* **7,** 495–501
45. Georgescu, M. M., Kirsch, K. H., Akagi, T., Shishido, T., and Hanafusa, H. (1999) *Proc. Natl. Acad. Sci. U. S. A.* **96,** 10182–10187
46. Naganuma, A., Nozaki, A., Tanaka, T., Sugiyama, K., Takagi, H., Mori, M., Shimotohno, K., and Kato, N. (2000) *J. Virol.* **74,** 8744–8750
47. Hijikata, M., Mizushima, H., Akagi, T., Mori, S., Kakiuchi, N., Kato, N., Tanaka, T., Kimura, K., and Shimotohno, K. (1993) *J. Virol.* **67,** 4665–4675
48. Efthymiadis, A., Shao, H., Hubner, S., and Jans, D. (1997) *J. Biol. Chem.* **272,** 22134–22139
49. Nozaki, A., and Kato, N. (2002) *Acta Med. Okayama* **56,** 107–110
50. Spik, G., Coddeville, B., and Montreuil, J. (1988) *Biochimie (Paris)* **70,** 1459–1469
51. Powell, M. J., and Ogden, J. E. (1990) *Nucleic Acids Res.* **18,** 4013–4013
52. Huang, K. X., Huang, Q. L., Wilduang, M. R., Croteau, R., and Scott, A. I. (1998) *Protein Expr. Purif.* **13,** 90–96
53. Kato, N., Nozaki, A., Naganuma, A., Ikeda, M., and Tanaka, K. (2000) *Curr. Top. Biochem. Res.* **3,** 164–173
54. Oren, R., Takahashi, S., Doss, C., Levy, R., and Levy, S. (1990) *Mol. Cell. Biol.* **10,** 4007–4015
55. Petracca, R., Falugi, F., Galli, G., Norais, N., Rosa, D., Campagnoli, S., Burgio, V., Di Stasio, E., Giardina, B., Houghton, M., Abrignali, S., and Grandi, G. (2000) *J. Virol.* **74,** 4824–4830
56. Flint, M., Maidens, C., Loomis-Price, L. D., Shotton, C., Dubuisson, J., Monk, P., Higginbottom, A., Levy, S., and McKeating, J. A. (1999) *J. Virol.* **73,** 6235–6244
57. Higginbottom, A., Quinn, E. R., Kuo, C. C., Flint, M., Wilson, L. H., Bianchi, E., Nicosia, A., Monk, P. N., McKeating, J. A., and Levy, S. (2000) *J. Virol.* **74,** 3642–3649
58. Takikawa, S., Ishii, K., Aizaki, H., Suzuki, T., Asakura, H., Matsuura, Y., and Miyamura, T. (2000) *J. Virol.* **74,** 5066–5074
59. Deleersnyder, V., Pillez, A., Wychowski, C., Blight, K., Xu, J., Hahn, Y. S., Rice, C. M., and Dubuisson, J. (1997) *J. Virol.* **71,** 697–704
60. Yi, M. K., Nakamoto, Y., Kaneko, S., and Murakami, S. (1997) *Virology* **231,** 119–129

Available online at www.sciencedirect.com
SCIENCE DIRECT®
Biochemical and Biophysical Research Communications 306 (2003) 756–766
BBRC
www.elsevier.com/locate/ybbrc

Establishment of a hepatitis C virus subgenomic replicon derived from human hepatocytes infected in vitro☆

Nobuyuki Kato,[a,*] Kazuo Sugiyama,[b] Katsuyuki Namba,[a,c] Hiromichi Dansako,[a,d] Takashi Nakamura,[a] Marika Takami,[a] Kazuhito Naka,[a] Akito Nozaki,[a] and Kunitada Shimotohno[e]

[a] *Department of Molecular Biology, Okayama University Graduate School of Medicine and Dentistry, 2-5-1 Shikata-cho, Okayama 700-8558, Japan*
[b] *Virology Division, National Cancer Center Research, Institute, 5-1-1 Tsukiji, Chuo-ku, Tokyo 104-0045, Japan*
[c] *First Department of Internal Medicine, Okayama University Graduate School of Medicine and Dentistry, 2-5-1 Shikata-cho, Okayama 700-8558, Japan*
[d] *Department of Internal Medicine II, Okayama University Graduate School of Medicine and Dentistry, 2-5-1 Shikata-cho, Okayama 700-8558, Japan*
[e] *Department of Viral Oncology, Institute for Virus, Research, Kyoto University, 53 Kawara-cho Shogo-in, Sakyo-ku, Kyoto 606-8507, Japan*

Received 16 May 2003

Abstract

The hepatitis C virus (HCV) replicon system is a potent tool for understanding the mechanisms of HCV replication and proliferation, and for the development of treatments for patients with HCV. Recently, we established an HCV subgenomic replicon (50-1) using HCV genome RNA obtained from the cultured human T cell line MT-2C infected with HCV (isolate 1B-1) in vitro. In order to further obtain other HCV replicons without difficulty, we generated a replicon RNA library derived from human non-neoplastic hepatocytes infected with HCV (isolate 1B-2) in vitro. Upon transfection of the generated RNA library to "cured cells," from which the 50-1 subgenomic replicon was eliminated by prolonged treatment with interferon-α, we successfully established a new HCV subgenomic replicon, 1B-2R1. We characterized 1B-2R1 replicon in terms of efficiency of replication, HCV sequence, and sensitivity to interferons. The results revealed that the replication level of the 1B-2R1 replicon was comparable to that of the 50-1 replicon. We also found that the 1B-2R1 replicon possessed an HCV sequence distinct from those of other replicons established to date, and that the 1B-2R1 replicon was sensitive to interferon-α, interferon-β, and interferon-γ. Taken together, present results indicate that the replicon RNA library generated using an in vitro HCV infection system is useful for the establishment of an HCV subgenomic replicon.

Keywords: Hepatitis C virus; PH5CH8; Huh-7; Replication; Replicon; Interferon

Hepatitis C virus (HCV) infection frequently causes chronic hepatitis [1,2] and progresses to liver cirrhosis and hepatocellular carcinoma [3,4]. HCV is an enveloped, positive, single stranded-RNA (9.6-kb) virus belonging to the family *Flaviviridae* [5,6]. The HCV genome shows remarkable genetic heterogeneity, and to date at least six major HCV genotypes (1–6), which have been further grouped into more than 50 subtypes, have been identified [7,8]. The HCV genome encodes a large polyprotein precursor of approximately 3000 amino acid residues, and this precursor protein is cleaved by the host and viral proteinases to generate at least 10 proteins in the following order: NH_2-core-envelope 1-envelope 2-p7-non-structural protein 2 (NS2)-NS3-NS4A-NS4B-NS5A-NS5B-COOH [9–11].

Although many issues have been addressed over the past decade regarding viral genomes and the functions of the viral proteins [12,13], the lack of reproducible and efficient HCV proliferation in cell cultures [14] has been a serious handicap to fighting this disease. However, in

☆ The nucleotide sequence data reported in this paper will appear in the DDBJ, EMBL, and GenBank nucleotide sequence databases under Accession No. AB109543.

* Corresponding author. Fax: +81-86-235-7392.
E-mail address: nkato@md.okayama-u.ac.jp (N. Kato).

0006-291X/03/$ - see front matter © 2003 Elsevier Science (USA). All rights reserved.
doi:10.1016/S0006-291X(03)01047-7

1999, a strategy was established for the development of an HCV-cell culture propagation system, i.e., Con1-derived HCV subgenomic selectable replicons containing the NS2–NS5B or the NS3–NS5B regions were established using a human hepatoma cell line, Huh-7 [15]. Since that discovery, additional Con1-derived [16], N-derived [17], and H77-derived [18] subgenomic replicons have also been established using either HCV genome isolated from human liver tissues chronically infected with HCV or by using another source of HCV genome, the RNA transcript of which was confirmed to be infectious when inoculated into the liver of a chimpanzee. To allow for the selection of only those cells in which HCV will efficiently replicate, a neomycin phosphotransferase (neo^r) gene was introduced downstream of the HCV internal ribosome entry site (IRES) instead of the structural protein-encoding region. A second encephalomyocarditis virus (EMCV) IRES was also used to allow for the production of the HCV NS proteins. In this system, replicated HCV RNAs were detected by Northern blot analysis and the HCV proteins that were produced were detected by Western blot analysis [15–18]. Treatment of replicon-containing cells with interferon (IFN)-α [19,20] and IFN-γ [21] is known to produce a remarkable decrease in subgenomic HCV RNA, albeit by unknown mechanisms. Although this subgenomic replicon system cannot produce the HCV virion itself, it is very useful for the study of the HCV replication mechanism and for the development of antiviral reagents. Furthermore, genome-length HCV replicons containing full-length HCV polyprotein were also recently produced using Huh-7 cells [17–22], although the production of infectious HCV from the genome-length HCV replicons has not been demonstrated to date.

We previously reported that the human T cell line MT-2C [23] and the human hepatocyte cell line PH5CH8 [24] were susceptible to HCV infection and supported HCV replication, although HCV proliferation occurred at a fairly low level; in that study, we also reported that the limited HCV populations among those in the inocula became predominant in these cells during culture after inoculation [25,26], suggesting that the replicable HCV genomes were selected upon infection of these cells and that these HCV genomes are good replicon candidates. According to our hypothesis, we recently succeeded at establishing an HCV subgenomic replicon (50-1) using an HCV RNA clone obtained from MT-2C cells infected with HCV (isolate 1B-1) [27]. This result indicated that our strategy was useful for the establishment of an HCV replicon.

As mentioned above, four different HCV subgenomic replicons derived from three isolates (Con1, N, and 1B-1) belonging to genotype 1b and from one isolate (H77) belonging to genotype 1a have been established to date. However, in order to facilitate the study of HCV, it was necessary to obtain additional replicons derived from different HCV isolates, because HCV genomic sequences are known to be highly diverse among HCV isolates [7,8], and are known to show several functional differences between isolates, including IFN sensitivity [28] and translational activity of the IRES [29], even among different isolates of the same genotype [30]. In addition, the replicons established thus far have been derived from limited genomic sequences of HCV, therefore, there remains some concern that those HCV sequences might be defective or limited in some manner.

In order to efficiently obtain HCV replicons, we generated a replicon RNA library, which was derived from PH5CH8 cells infected with HCV (isolate 1B-2) in vitro. Here, we report a new HCV subgenomic replicon (1B-2R1) that was selected from this replicon RNA library; 1B-2R1 is compared with other established subgenomic replicons.

Materials and methods

Cell cultures. Simian virus 40 large T antigen-immortalized non-neoplastic human PH5CH8 hepatocytes were maintained as described previously [31]. Huh-7 cells were cultured in Dulbecco's modified Eagle's medium supplemented with 10% fetal bovine serum.

Virus inoculation. Virus inoculation was performed by a previously described method [26]. Briefly, a total of 100 μl of undiluted serum 1B-2 containing about 10^7 HCV (1b genotype) per ml was added to PH5CH8 cells (5×10^6 cells) suspended in 1 ml of fresh culture medium, and the cells were incubated for 7 h at 37 °C. After washing the cells three times with 1 ml PBS, they were cultured with 10 ml of fresh medium at 32 °C for 8 days [23] and then the cells were harvested for the PCR amplification of the HCV RNA.

Reverse transcription (RT)-PCR and RT-nested PCR. RNAs from the cultured cells were prepared using the RNeasy extraction kit (Qiagen). The RNA samples (0.5–2 μg) served as templates for RT using SuperScript II (Invitrogen). For the amplification of the NS3–NS5B regions of HCV RNA from the HCV-infected PH5CH8 cells, RT-nested PCR was performed separately in two parts; one part covered NS3 region to most of the NS4B region and the other part covered the carboxyl portion of the NS4B region to NS5B region (Fig. 1). For the former part, the antisense primer 301RA, 5′-CAACACC GTGCATATCCAGTCCCA-3′ (corresponding to positions 6282–6305 of the HCV genome), was used for RT. Primers 542, 5′-GTAGA GCCCGTCGTCTTCTCTGACATGGA-3′ (corresponding to positions 3252–3280 of the HCV genome), and 301RA were employed in the first round of PCR (35 cycles). An internal primer pair (538: 5′-CATCATCACTAGTCTCACAGGCCGGGACAGGAAC-3′ and 546R: 5′-CACGCGCGGCCGCGTCGCTCTCAGGCACATAGTG CGTGGG-3′; corresponding to positions 3467–3500 and positions 6132–6171 of the HCV genome, and containing a *SpeI* and a *NotI* recognition site (underlined), respectively) was used for the second round of PCR (35 cycles). The PCR yielded a 2731 bp amplified product. For the latter part, the antisense primer 386R, 5′-AATG GCCTATTGGCCTGGAG-3′ (corresponding to positions 9390–9409 of the HCV genome), was used for RT. Primers 548 (5′-GCT GTGCAGTGGATGAACCGGCTGATAGC-3′, corresponding to positions 6075–6103 of the HCV genome) and 419R (5′-GAGTGT TTAGCTCCCCGTTCACCGGTTGG-3′, corresponding to positions 9364–9392 of the HCV genome) were employed in the first round of PCR (35 cycles). An internal primer pair (547, 5′-GCGAC GCGGCCGCGCGTGTCACTCAGATCCTCTCCAGCCTTACCA T-3′ and 541R, 5′-AGCTTGGTCCGTACGGCCCAGTTGAAGA

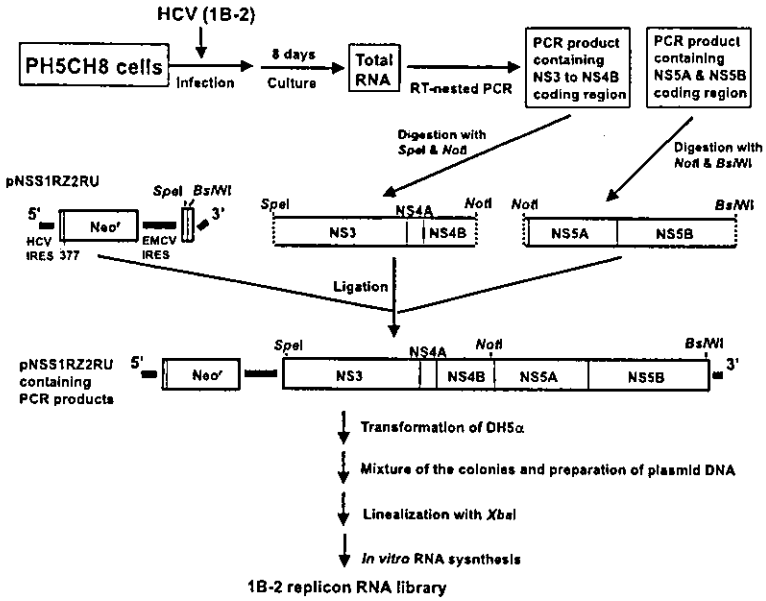

Fig. 1. Outline for the construction of the 1B-2 replicon RNA library. Two RT-nested PCR products (the NS3 region to the NS4B region, and the NS5A region to the NS5B region) obtained using total RNA derived from HCV (1B-2 isolate)-infected PH5CH8 cells were ligated to the *Spe*I and *Bsi*WI sites of pNSS1RZ2RU, as described in Materials and methods. The region from nucleotide positions 1–377 in the HCV genome was used as the 5′-terminal structure including the HCV IRES region in this replicon.

GGTACTTG-3′; corresponding to positions 6154–6193 and positions 9164–9199 of the HCV genome, and containing a *Not*I and a *Bsi*WI recognition site (underlined), respectively) was used for the second round of PCR (35 cycles). The PCR yielded a 3074 bp amplified product. KOD-plus DNA polymerase (Toyobo, Japan) was used as a proofreading enzyme [32] for the PCR, and each PCR cycle consisted of annealing at 55 °C for 45 s, primer extension at 68 °C for 4 min, and denaturation at 94 °C for 40 s. For the amplification of HCV subgenomic replicon RNA from 1B-2R1 replicon cells, RT-PCR was also performed separately in two parts; one part covered 5′-untranslated region (UTR) to the amino terminal of the NS3 region and the other part covered the NS3 region to NS5B region (see Fig. 4A). For the former part, the antisense primer 290R, 5′-TCAACCTGGTTCT TGTCCCG-3′ (corresponding to positions 3489–3508 of the HCV genome), was used for RT. Primers 21X, 5′-ATTATTCTAGAGCCA GCCCCCGATTGGGGGCG-3′ [corresponding to positions 1–21 of the HCV genome, and containing a *Xba*I recognition site (underlined)] and EMCVIRESRX, 5′-ATTATTCTAGAGACCTGTGAGGCTGG TGATGATGC-3′ [corresponding to positions 3466–3489 of the HCV genome, and containing a *Xba*I recognition site (underlined)] were used for the PCR (35 cycles). The PCR yielded a 2033 bp amplified product. For the latter part, the antisense primer 386R was used for RT. Primers pNNRZ2SX, 5′-ATTATTCTAGACATGCTTTACATGTG TTTAGTCGAGG-3′ [locating within EMCV IRES, and containing a *Xba*I recognition site (underlined)] and 9388RX, 5′-ATTATTCTAGA vATGGCCTATTGGCCTGGAGTG-3′ [corresponding to positions 9388–9409 of the HCV genome, and containing a *Xba*I recognition site (underlined)], were used for the PCR (35 cycles). The PCR yielded a 6107 bp amplified product. KOD-plus DNA polymerase (Toyobo, Japan) was used as a proofreading enzyme for PCR, and each PCR cycle consisted of annealing at 60 °C for 45 s, primer extension at 68 °C for 2.5 min (for 2033 bp) and 7 min (for 6107 bp), and denaturation at 94 °C for 15 s. The PCR products (2033 and 6107 bp) were used for the sequence analysis.

Replicon cassette plasmid. Two mutations were introduced by a PCR technique into a previously constructed plasmid, pNNRZ2RU [27], giving a *Spe*I (ACTAGT) sequence in the 5′ part of the NS3 region that corresponded to positions 3474–3479 (ACCAGC) of the HCV isolate MILD (Accession No. AB080299). A *Bsi*WI (CGTACG) sequence was also created in the 3′ part of the NS5B region, resulting in the construct pNNSS1RZ2RU. The *Spe*I–*Bsi*WI fragment was removed from pNNSS1RZ2RU by digestion with the corresponding restriction enzymes, and then a linker (annealed with oligomers 5′-C TAGTAATGCGGCCGCTGTC-3′ and 5′-GTACGACAGCGGCCG CATTA-3′) was inserted into that position, generating replicon cassette plasmid pNSS1RZ2RU (Fig. 1).

Generation of a replicon RNA library. Two PCR products (2731 bp containing the NS3–NS4B regions, and 3074 bp containing the NS5A and NS5B regions, see Fig. 1), were obtained using the total RNA from the HCV-infected PH5CH8 cells. These PCR products were digested with *Spe*I and *Not*I in case of the former (2731 bp), and *Not*I and *Bsi*WI in case of the latter (3074 bp). Then, both digested PCR products were simultaneously ligated into the plasmid pNSS1RZ2RU, which was predigested with *Spe*I and *Bsi*WI. One hundred microlitres of *Escherichia coli*, competent high DH5α (Invitrogen), was transformed using the ligation reaction mixture according to the manufacturer's protocol. The transformed DH5α cells were seeded onto two 9-cm LB plates containing ampicillin (50 μg/ml) and the cultures were incubated overnight at 37 °C, resulting in the generation of a number of colonies. Five millilitres of LB medium containing ampicillin (50 μg/ml) was added onto each of the plates bearing colonies. The medium was collected after it was gently shaken at room temperature for 30 min. The collected LB medium was added to 100 ml of new LB medium containing ampicillin (50 μg/ml); the cultures were then incubated for 6 h at 30 °C. Plasmid DNA prepared with a Plasmid Midi kit (Qiagen) was digested with *Xba*I and subjected to 1% separative agarose gel electrophoresis. After staining the gel with ethidium bromide, a band of 12.6 kbp (the expected size of the linealized form of pNSS1RZ2RU possessing the NS3–NS5B regions) was excised from the gel and was purified using a Gel Extraction kit (Qiagen). Finally, a purified 12.6 kbp fragment was used as the template for in vitro RNA synthesis using a MEGAscript T7 kit (Ambion). The RNA (approximately 8 kb in length) was then synthesized according to the manufacturer's protocol and was used as a replicon RNA library for the RNA transfection to Huh-7 cells.

RNA transfection and selection of G418-resistant cells. RNA transfection to Huh-7 cells was performed by electroporation, as

described by Lohmann et al. [15]. Selection of cells was performed in complete DMEM with 300 μg/ml G418 (Geneticine, Invitrogen).

PCR. Genomic DNA from the cultured cells was purified using the Wizard SV genomic DNA purification system (Promega). One microgram of genomic DNA was subjected to PCR for the detection of the HCV 5′-UTR and the IFN-β gene. For the detection of the HCV 5′-UTR, two sets of primers were used for the PCR (35 cycles). The first set of primers was 196, 5′-CCATGGCGTTAGTATGAGTG-3′ (corresponding to positions 83–102 of the HCV genome) and 319R, 5′-TGCTCATGGTGCACGGTCTA-3′ (corresponding to positions 329–348 of the HCV genome); the second set of primers was 426, 5′-CCG ATTGGGGGCGACACTCCACC-3′ (corresponding to positions 9–31 of the HCV genome) and 450R, 5′-GAGCGGGTTAATCCAA GAAAGGAC-3′ (corresponding to positions 190–213 of the HCV genome). For the detection of the IFN-β gene (Accession No. V00547), the following primers were used for the PCR (35 cycles): IFN-β-5′, 5′-C CCTGAGGAGATTAAGCAGCTGC-3′ and IFN-β-3′, 5′-AGTTC CTTAGGAvTTTCCACTCTGAC-3′. KOD-plus DNA polymerase (Toyobo, Japan) was used for the PCR, and each PCR cycle consisted of annealing at 60 °C for 45 s, primer extension at 68 °C for 1 min, and denaturation at 94 °C for 10 s. Ten pg of pM1LE [27] containing the full-length HCV genome sequence was used as template DNA in the positive control for the detection of the HCV 5′-UTR. PCR without template DNA was also performed as a negative control. The PCR products (266 and 205 bp for the HCV 5′-UTR and 341 bp for the IFN-β gene) were detected by staining with ethidium bromide after 3% agarose gel electrophoresis.

Northern blot analysis. Three micrograms of total RNA from the cultured cells was used for the detection of HCV subgenomic replicon RNA and β-actin. Northern blotting and hybridization were performed as described previously [33,34]. To confirm the quality of the RNA, 28S and 18S ribosomal RNAs were stained with ethidium bromide. After blotting samples onto a Hybond-XL nylon membrane, the membrane was cut approximately 1 cm below the 28S ribosomal RNA band, and the upper strip containing the HCV subgenomic replicon RNA was hybridized with a DIG-labeled negative-sense RNA probe complementary to the NS5B region (positions 8935–9374 of the HCV genome). The lower strip that was hybridized with a β-actin-specific DIG-labeled antisense RNA probe was used to check the amount of RNA that had been loaded in each lane of the gel. The DIG Northern Starter Kit (Roche) was used to generate the DIG-labeled, single-stranded RNA probes, according to the manufacturer's protocol. As a molecular length marker, the RNA ladder (Invitrogen) was utilized.

Western blot analysis. The preparation of cell lysates, sodium dodecyl sulfate–polyacrylamide gel electrophoresis (SDS–PAGE), and immunoblotting analysis with a polyvinylidene difluoride membrane were performed as previously described [10,34]. The antibodies used in this study were those against NS3 (Novocastra Laboratories, UK), anti-NS5A [10], anti-NS5B (a generous gift from M. Kohara, Tokyo Metropolitan Institute of Medical Science), and β-actin (Sigma). Immunocomplexes on the filters were detected by enhanced chemiluminescence assay (Renaissance; Perkin–Elmer Life Sciences).

IFN treatment. HCV subgenomic replicon cells (1×10^5) were plated at least in duplicate onto 6-well plates. Cells were cultured for 1 day before IFN treatment. Human IFN-α (Sigma), IFN-β (a gift from Toray Industries), and IFN-γ (Sigma) were added to the cells at a final concentration of 100 IU/ml and incubation was continued. The cells were harvested at 24 and 48 h after IFN treatment for the semi-quantitative HCV RNA analysis, or they were harvested at 6 days after IFN treatment for the Western blot analysis of HCV proteins.

Quantification of HCV subgenomic replicon RNA. Semi-quantitative analysis of HCV subgenomic replicon RNA was performed by the modification of a previously described method [23]. Briefly, 0.5 μg of the RNA prepared from the HCV subgenomic replicon cells was used for RT with SuperScript II using primer 319R. The synthesized cDNA was amplified by *Taq* DNA polymerase (Takara, Japan) using primers 319R and 196, resulting in a PCR product of 266 bp. PCR products (25 cycles) were detected by staining with ethidium bromide after 3% agarose gel electrophoresis. The intensity of the bands stained with ethidium bromide was quantified by a ChemiImager 4400 (Alpha Inotech). The amount of HCV replicon RNA was estimated by comparison with the pattern of gradual amplification obtained by using in vitro synthesized HCV RNA containing the 5′-UTR, as shown previously [23].

cDNA cloning and sequencing. PCR products containing 1B-2R1 subgenomic replicon sequences were digested with *Xba*I and then subcloned into the *Xba*I site of pBR322MC [27], which was derived from pBR322 and contained the multi-cloning site of pUC19, as described previously [35]. Plasmid inserts were sequenced in both the sense and antisense directions using Big Dye terminator cycle sequencing on an ABI PRISM 310 genetic analyzer (Applied Biosystems).

Results

Construction of a replicon RNA library

We recently succeeded at establishing an HCV subgenomic replicon (50-1) using an HCV genomic clone obtained from HCV (isolate 1B-1)-infected MT-2C cells, suggesting that the use of an in vitro HCV infection and proliferation culture system is useful for the selection of replicable HCV genomes [27]. Since all HCV subgenomic replicons that have been reported to date [15–18,27] were derived from cloned HCV sequences, and were established by overcoming several difficulties, thus it was expected to be difficult to establish a new subgenomic replicon using only a single HCV clone obtained from a different HCV isolate. This expected difficulty led us to create a replicon RNA library derived from in vitro HCV-infected human cells.

The source of our replicon RNA library was a human hepatocyte PH5CH8 cell line, which is susceptible to HCV infection and supports HCV replication [24]. PH5CH8 cells were inoculated with HCV-positive serum (isolate 1B-2), and at 8 days post-infection, total RNA was isolated from the cultured cells in order to amplify the HCV genomes that had replicated in the cells. The NS3–NS5B regions of the HCV genomes (separated into two parts; Fig. 1) were amplified by RT-nested PCR using a proofreading DNA polymerase [32]. Two obtained PCR products (*Spe*I and *Not*I digested fragment containing the NS3 region to most of NS4B region, and *Not*I and *Bsi*WI digested fragment containing the carboxyl part of the NS4B to NS5B region) were ligated into the *Spe*I and *Bsi*WI sites of a replicon cassette plasmid (pNSS1RZ2RU), which was constructed from pNNSS1RZ2RU [27] with two mutations introduced by PCR, as described in Materials and methods. Fig. 1 gives the outline of the construction of the replicon RNA library used in this study. The structure of the replicon RNA was basically the same as that of the 1B-1-derived replicon RNA [27], i.e., both

contained the 5′-UTR, the first 36 nucleotides of the core region, the NS3–NS5B regions, the 3′-UTR of the HCV genome, and the neo^r gene and EMCV IRES to be inserted into the region downstream of the short stretch of the core region, as shown in Fig. 1. We confirmed the nucleotide sequences of the boundary regions of the *Spe*I, *Not*I, and *Bsi*WI sites of the obtained pNSS1RZ2RU containing the NS3–NS5B regions. Based on the number of colonies of *E. coli* grown on the plates, it has been estimated that the obtained plasmids contained several hundred species of HCV genomes. RNA was synthesized with a MEGAscript T7 kit in vitro using a pNSS1RZ2RU containing the NS3–NS5B regions linealized by digestion with *Xba*I as a template. The synthesized RNA transcript (8.1 kb in length) was used as a replicon RNA library.

Establishment of 1B-2-derived G418-resistant cells

A constructed replicon RNA library was first transfected into Huh-7 cells by electroporation and the G418-resistant cells were selected as described previously [15,27]. However, we were unable to obtain any G418-resistant colonies, although several G418-resistant colonies were obtained from cells transfected with the total RNA derived from 50-1 subgenomic replicon cells (data not shown). We considered that the lack of replication might have been due to the Huh-7 cellular environment. During the course of this study, Blight et al. [18] reported that a Con1 subgenomic replicon could be eliminated from the cells by prolonged treatment with IFN-α and that a majority of these "cured cells" allowed for HCV RNA replication. That report led us to use cured cells, from which the subgenomic replicon was eliminated by treatment with IFN-α, for additional experiments. The 50-1 subgenomic replicon cells were cultured without G418 with prolonged treatment of IFN-α (3000 IU/ml); as a consequence, we were able to obtain cured cells by confirming that HCV RNA was not detected by RT-PCR (data not shown).

In order to obtain subgenomic replicon cells, the replicon RNA library was then transfected into the cured cells by electroporation. Following 20 days of culturing in the presence of G418, two colonies (one large and the other small) were obtained. The G418-resistant large colony was successfully proliferated; this colony was referred to as 1B-2R1, although we failed to achieve the proliferation of the G418-resistant small colony. 1B-2R1 cells showed a similar growth rate to that of the 50-1 subgenomic replicon cells in the presence of G418 (data not shown). Furthermore, we confirmed the complete cell death of the 1B-2R1 cells with the prolonged treatment of IFN-α (1000 IU/ml) in the presence of G418, suggesting that RNA-based expression of the neo^r gene product is occurring in the 1B-2R1 cells.

Detection of the subgenomic RNA maintained in 1B-2R1 cells

To exclude the possibility that a replicon RNA sequence had integrated into the genomic DNA, we examined the presence of the HCV 5′-UTR sequence in the genomic DNA isolated from 1B-2R1 cells by PCR. 50-1 replicon cells and the cured cells were also examined for the comparison. As shown in Fig. 2A, PCRs using two primer sets for the detection of the HCV 5′-UTR (266 and 205 nucleotides) did not detect the HCV 5′-UTR sequence in the genomic DNAs from the 1B-2R1 cells, the 50-1 replicon cells, and the cured cells, although the expected PCR products were obtained when pMILE containing the full-length HCV genomic sequence was used as a template for the PCR. To test the efficiency of the PCR analysis and the quality of the genomic DNAs, a set of primers was used for the PCR detection of an intronless IFN-β gene (1 copy per haploid genome). The

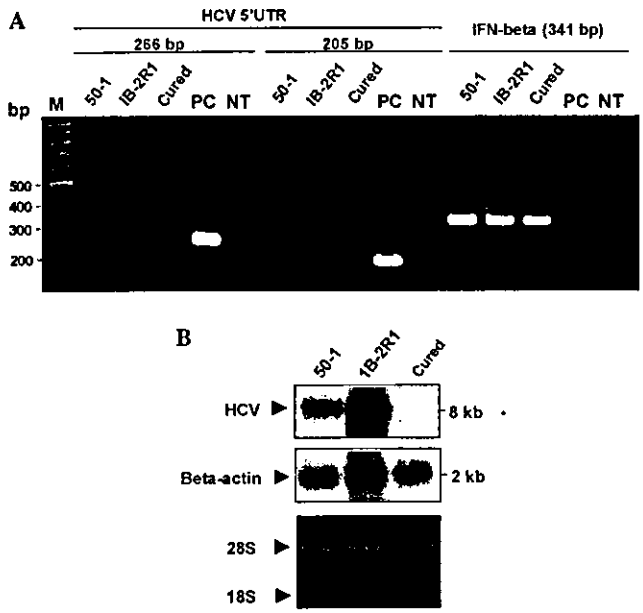

Fig. 2. Characterization of 1B-2R1 cells. (A) The replicon-derived sequences were not integrated in the genomic DNA from 1B-2R1 cells. Genomic DNAs from the 1B-2R1 and 50-1 cells, and genomic DNA from the cured cells, were subjected to PCR for the detection of the HCV 5′-UTR and the IFN-β gene. pMILE [27] containing the full-length HCV genome sequence was used as a template DNA for a positive control (lane PC) of the HCV 5′-UTR. PCR was performed without the template DNA as a negative control (lane NT). PCR products (266 and 205 bp for the HCV 5′-UTR, and 341 bp for the IFN-β gene) were detected by staining with ethidium bromide after 3% agarose gel electrophoresis. Lane M, the 100 bp DNA ladder served as a size marker. (B) Detection of HCV subgenomic RNA in 1B-2R1 cells. Total RNAs from the 1B-2R1 and 50-1 cells, as well as RNA from the cured cells, were analyzed by Northern blotting using a positive-stranded HCV genome-specific RNA probe (upper panel) and a β-actin-specific RNA probe (middle panel), and RNA samples were equalized for 28S and 18S ribosomal RNAs stained with ethidium bromide (lower panel). The positions of HCV subgenomic replicon RNA, β-actin mRNA, and ribosomal RNAs (28S and 18S) are indicated by arrowheads.

results revealed that the expected PCR products (341 bp) were detected in the genomic DNAs from the 50-1 replicon cells, the 1B-2R1 cells, and the cured cells (Fig. 2A). These results indicated that at least the HCV 5′-UTR sequence, which is critical for the translation of the neo^r gene, was not present in either the genomic DNA from 1B-2R1 cells or in that from 50-1 replicon cells.

To confirm the presence of subgenomic RNA in the 1B-2R1 cells, Northern blot analysis was carried out using an antisense strand sequence of the NS5B region in the HCV genome as a probe. As shown in Fig. 2B, the presence of a substantial abundance of HCV-specific RNA with a length of approximately 8 kb was detected in the extracts of total cellular RNA prepared from the 1B-2R1 cells, but not in the RNA from the cured cells. The amount of 1B-2R1 subgenomic RNA in the cells was greater than that of the 50-1 subgenomic replicon RNA (Fig. 2B). This result suggests that HCV subgenomic RNA is efficiently maintained in 1B-2R1 cells.

Detection of HCV NS proteins produced in 1B-2R1 cells

To determine the level of HCV proteins produced from 1B-2R1 subgenomic replicon RNA, Western blot analysis was carried out using antibodies against HCV NS proteins. As shown in Fig. 3, NS3, NS5A, and NS5B proteins were detected in the cell lysates of 1B-2R1 cells as well as in the lysates of 50-1 replicon cells, but these proteins were not found among the lysates of the cured cells. The sizes of these NS proteins in 1B-2R1 cells were the same as those in the 50-1 replicon cells (Fig. 3 and [27]), and were also the same as those discussed in a previous report [10]. The expression levels of NS3 and NS5A, but not those of NS5B, in 1B-2R1 cells were somewhat higher than those in 50-1 replicon cells.

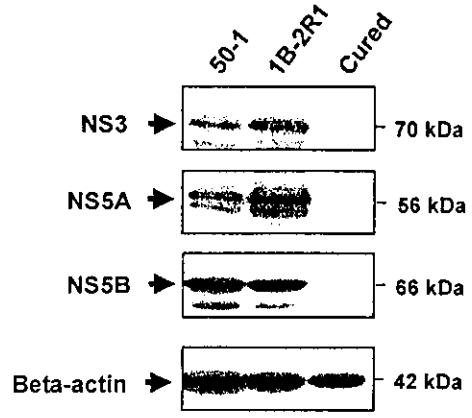

Fig. 3. Detection of HCV NS proteins produced in 1B-2R1 cells. Production of NS3, NS5A, and NS5B in 1B-2R1 cells was analyzed by immunoblotting using anti-NS3, anti-NS5A, and anti-NS5B antibodies, respectively, as described previously [10]. The results were compared with those from 50-1 replicon cells. β-Actin was used as a control for the amount of protein loaded per lane. The band corresponding to each NS protein is indicated by an arrowhead.

Taken together, these results indicate that 1B-2-derived subgenomic RNA efficiently replicates in 1B-2R1 cells, and that the replication level of the 1B-2R1 subgenomic replicon is equivalent to or more than that of the 50-1 subgenomic replicon.

Genetic analysis of the 1B-2R1 replicon and its comparison with other replicons

To confirm that the replicon sequence in 1B-2R1 cells was actually derived from HCV isolate 1B-2, and to exclude the possibility that 1B-2R1 replicon cells were derived from a small number of 50-1 replicon cells still remaining after IFN treatment, we carried out a genetic analysis of the 1B-2R1 subgenomic replicon RNA. Two separate RNA fragments (one 2.0 kb in length, containing 5′-UTR, the neo^r gene, and EMCV IRES; and the other 6.1 kb in length, containing the NS3 region to the NS5B region) were amplified by RT-PCR using proofreading KOD-plus DNA polymerase [32]. The fragments were then subcloned into pBR322MC, as shown in Fig. 4A. The nucleotide sequences of each of the three independent clones obtained were determined.

Regarding the first half (2.0 kb) of the 1B-2R1 subgenomic replicon RNA, the three obtained clones showed highly homologous nucleotide sequences. Two clones showed only one or two nucleotide differences from those of the consensus sequences obtained from these three clones, and the third clone was identical to the consensus sequences. The sequences of the first half of the 1B-2R1 subgenomic replicon RNA were almost the same as those of 50-1 subgenomic replicon RNA [27]. This result was not surprising, because we used the replicon cassette plasmid containing the same sequences as the replicon plasmid used for the establishment of 50-1 replicon cells, with the exception of the NS3–NS5B regions. However, interestingly, the three 1B-2R1 clones obtained substituted guanosine for adenosine at position 201 in the 5′-UTR.

The NS3–NS5B regions of the 1B-2R1 subgenomic replicon RNA were also highly homologous among the three clones sequenced. The nucleotide sequence diversity among the three clones was only 0.04%. The three clones showed only two or three nucleotide differences from the nucleotides in the consensus sequences obtained from these three clones. However, the 1B-2R1 consensus sequences of NS3–NS5B regions showed a differences of 8.1% from those of the 50-1 replicon RNA [27], indicating that 1B-2R1 replicon cells were not contaminated by the 50-1 replicon cells. Similarly, the sequences of the 1B-2R1 replicon RNA showed 8.1% and 9.0% nucleotide-sequence diversity compared with Con1 [15] and N [17] replicon RNAs, respectively. The nucleotide-sequence diversity between 1B-2R1 and the representative HCV isolate J (HCV-J [5]) was also 8.9%. These diversities in nucleotide sequences were within the same range

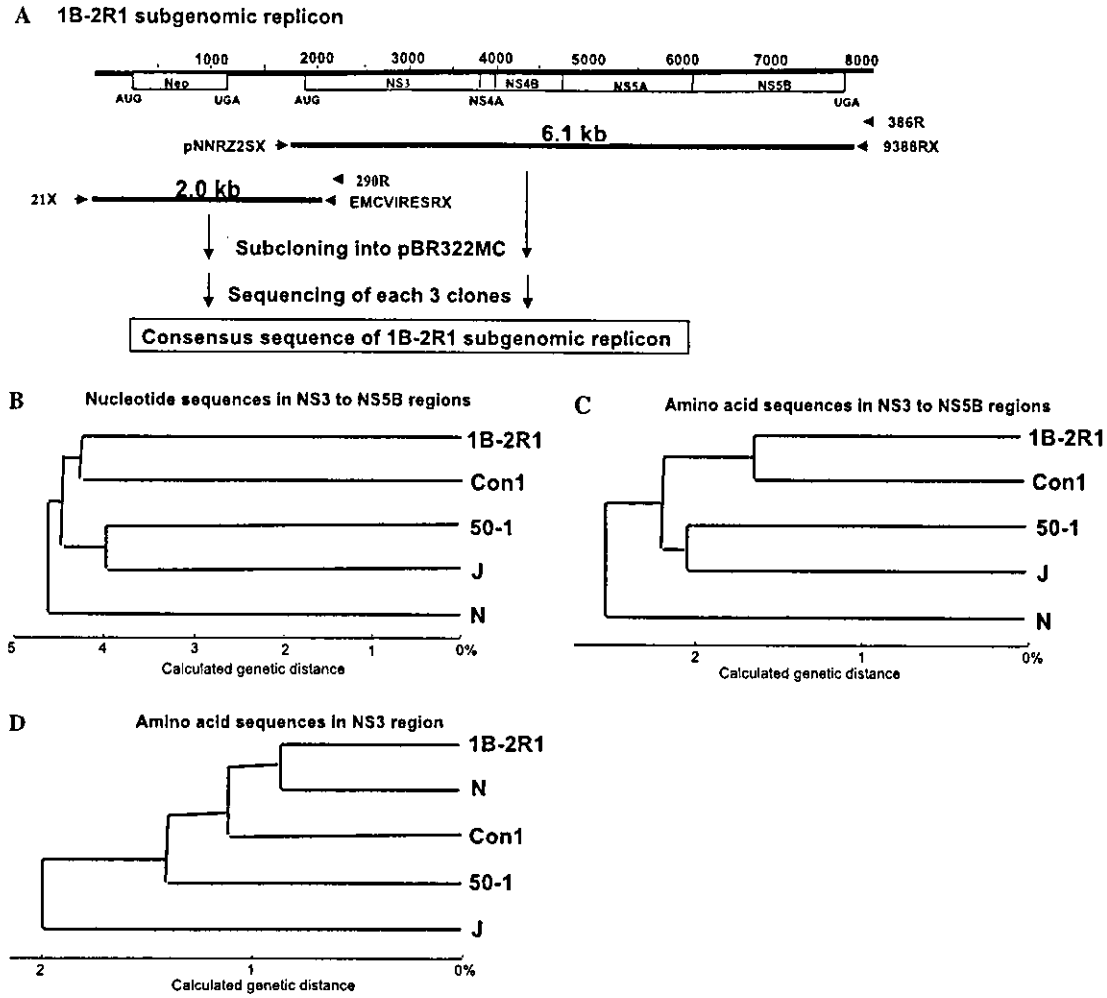

Fig. 4. Genetic analysis of the 1B-2R1 subgenomic replicon. (A) Outline of the genetic analysis of 1B-2R1 subgenomic replicon RNA. Two PCR products (2.0 and 6.1 kb) were ligated into the *XbaI* site of pBR322MC. Sequencing of each of the three clones was performed to obtain the consensus sequences of the 1B-2R1 replicon RNA. (B) A phylogenetic tree was created based on the nucleotide sequences of the NS3–NS5B regions, using the four subgenomic 1b replicons (Con1, N, 50-1, and 1B-2R1) and the HCV-J isolate. The GENETYX-MAC program, an unweighted pair-grouping method with arithmetic mean [36], was used for the analysis. (C) A phylogenetic tree based on the amino acid sequences of the NS3–NS5B regions of the four subgenomic 1b replicons (Con1, N, 50-1, and 1B-2R1) and the HCV-J isolate. (D) A phylogenetic tree based on the amino acid sequences of the NS3 region of the four subgenomic 1b replicons (Con1, N, 50-1, and 1B-2R1) and the HCV-J isolate.

as those found in isolates of the 1b genotype of HCV [7,8]. A phylogenetic tree was constructed by the multi-alignment analysis of the sequences of 1b subgenomic replicons reported to date; the tree was constructed with the GENETYX-MAC program, an unweighted pair-grouping method with the arithmetic mean [36]. This phylogenetic analysis revealed that the 1B-2R1 replicon was located at a distinct position among the 1b genotype replicons, and it was slightly closer to the Con1 replicon than to the other replicons (Fig. 4B). A similar observation was also made by comparison of the levels of amino acid sequences. The amino acid sequence diversity among the three sequenced 1B-2R1 clones was also very low (0.11%). The three clones had only two or three different amino acids from those of the consensus sequences obtained from these three clones. Although the amino acid sequences of the NS proteins of the 1B-2R1 replicon were highly homologous among three clones, 1B-2R1 consensus sequences of the NS proteins showed 3.9%, 3.2%, 4.7%, and 4.6% differences in their amino acid sequences from those of 50-1 replicon [27], Con1 replicon [15] and N replicon [17], and HCV-J isolate [5], respectively. These diversities in amino acid sequences were also within the same range as those found among isolates of the 1b genotype of HCV [7,8]. As shown in Fig. 4C, the phylogenetic tree constructed based on the amino acid sequences was similar to that based on the nucleotide sequences.

We previously reported the amino acid sequences of NS5A obtained from human cultured cells infected with HCV (1B-2 isolate) [34]. The amino acid sequences of NS5A of the 1B-2R1 replicon were almost the same as those of previously obtained NS5A [34]. These results suggest that the NS3–NS5B regions of the 1B-2R1

replicon RNA were derived from the 1B-2 isolate. However, as a characteristic sequence in the 1B-2R1 subgenomic replicon RNA, we found that nucleotide position 6939 (the number of the nucleotide in the HCV genotype 1b genome) substituted cytidine for adenosine, resulting in the substitution of arginine for serine at amino acid position 2200 in NS5A. The same substitution has been recently reported by Lanford et al. [37] as one of the adaptive mutations in the NS5A region of the Con1-based subgenomic replicon (discussed below).

Moreover, the phylogenetic tree based on the amino acid sequences of NS3 revealed that the 1B-2R1 replicon was similar to that of the N replicon, and that HCV-J, which is not a replicon sequence, was most distant from 1B-2R1 replicon (Fig. 4D). Such a phylogenetic tree was not obtained for the other NS proteins. The difference between 1B-2R1 and N replicons was only 11 out of the 631 amino acids of NS3, although a 28-amino acid difference was observed between the 1B-2R1 replicon and HCV-J. These observations may indicate that the somewhat favorable amino acids of NS3 lead to efficient replication in Huh-7 cells.

1B-2R1 and 50-1 replicons are sensitive to IFN-α, IFN-β, and IFN-γ

To date, all of the Con1- and N-based subgenomic replicons have been reported to be highly sensitive to IFN-α, because HCV RNA replication was rapidly inhibited in the presence of IFN-α [16,19,20,37], although the precise mechanism of this inhibition has not yet been clarified. It was recently reported that IFN-γ also decreased HCV RNA in Con1 replicon cells [21,37]. Therefore, we examined the sensitivities of our established subgenomic replicons, 1B-2R1 and 50-1, against IFN-α, IFN-β, and IFN-γ. As shown in Fig. 5A, Western blot analysis revealed that NS5B was drastically decreased in both 1B-2R1 and 50-1 replicon cells at 5 days after treatment with IFN-α, IFN-β, and IFN-γ (100 IU/ml each), suggesting that both replicons are also sensitive to these IFNs. Interestingly, weak bands corresponding to NS5B still remained in the IFN-treated 50-1 replicon cells, whereas no significant bands were observed in the IFN-treated 1B-2R1 replicon cells. This observation suggests that the 1B-2R1 replicon is more sensitive to IFNs than the 50-1 replicon.

The effects of IFNs on the 1B-2R1 and 50-1 replicons were also analyzed by semi-quantitative RT-PCR. Fig. 5B shows representative results regarding a time-course experiment in which the number of HCV replicon molecules was measured at 24 and 48 h after treatment with IFN-α, IFN-β, and IFN-γ (100 IU/ml each). The untreated 1B-2R1 and 50-1 replicon cells contained about 10^8 HCV replicon molecules per μg of total RNA during the course of the culture period (Fig. 5B; lane N). In contrast, the amount of HCV replicon RNA decreased

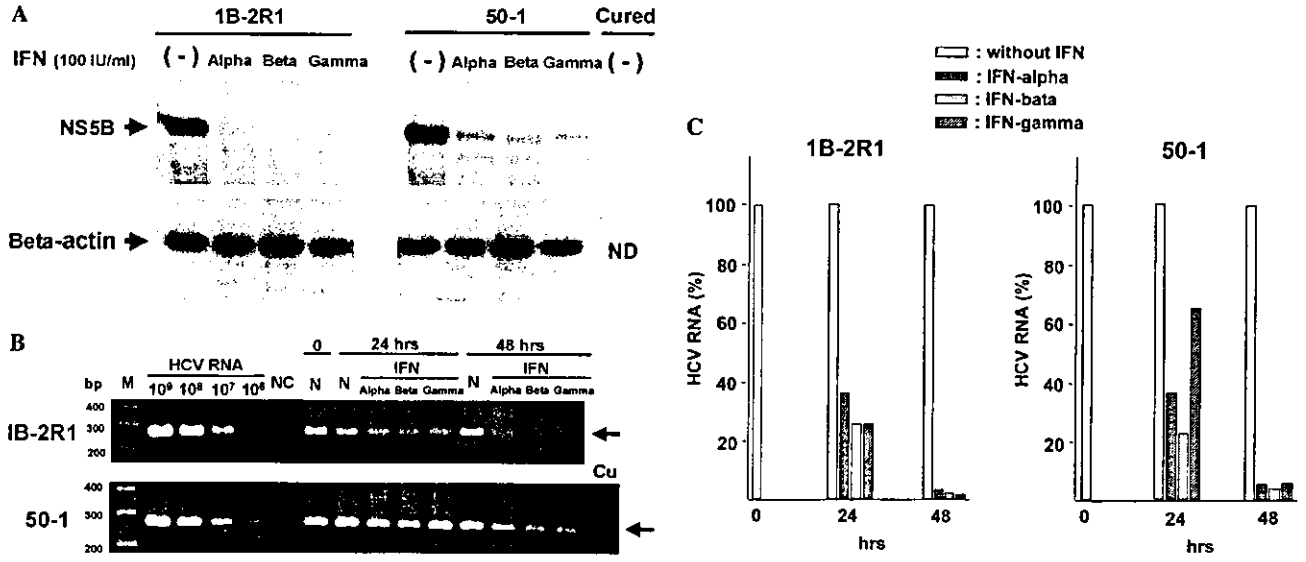

Fig. 5. IFN sensitivities of the 1B-2R1 and 50-1 subgenomic replicons. (A) Western blot analysis. 1B-2R1 and 50-1 replicon cells were treated with IFN-α, IFN-β, and IFN-γ (100 IU/ml each) for 5 days. The cured cells were used as control cells. NS5B was detected by immunoblot analysis using anti-NS5B antibodies. β-Actin was used as a control for the amount of protein loaded per lane. (B) RT-PCR analysis. 1B-2R1 and 50-1 replicon cells were treated with IFN-α, IFN-β, and IFN-γ (100 IU/ml each) for 24 and 48 h. The cured cells were used as control cells. The 5′-UTR of the HCV genome was detected by RT-PCR, as described in Materials and methods. In vitro synthesized positive-stranded HCV RNA containing the 5′-UTR (10^6–10^9 copies) was also subjected to RT-PCR as the standard in order to quantify the amount of subgenomic replicon RNA. The PCR product (266 bp) was detected by staining with ethidium bromide after 3% agarose gel electrophoresis. Representative results are shown. The positions of the PCR products are indicated by arrowheads. Lane M, the 100 bp DNA ladder used as a size marker; NC, no RNA; N, without IFN; Cu, the cured cells. (C) Semi-quantitative analysis. The intensities of bands stained with ethidium bromide on agarose gels, including those shown in (B), were quantified by a ChemiImager 4400. The data, obtained in more than duplicate assays, were averaged for the presentation.

in the IFN-treated cells within the first 24 h of treatment, and then further decreased to less than 10% of the level in the untreated cells during the next 24 h, regardless of the IFN species (Fig. 5B). We repeated these experiments more than twice, and the bands stained with ethidium bromide on the agarose gels were quantified as shown in Fig. 5C. The results revealed that the amount of 1B-2R1 replicon RNA decreased more sharply than that of the 50-1 replicon RNA after IFN treatment. In particular, the level of 50-1 replicon RNA in the cells at 24 h after IFN-γ treatment, but not IFN-α and IFN-β treatment, was still maintained at about 60% of the level in the untreated cells, whereas the level of 1B-2R1 replicon RNA decreased to about 30% of that of the untreated cells. Although 1B-2 and 50-1 replicons showed slightly different IFN-sensitivities, our study clarified that our established 1B-2R1 and 50-1 replicons belonging to the 1b genotype were also sensitive to IFN-α and IFN-γ, and we demonstrated for the first time that IFN-β also inhibited the replication of HCV subgenomic RNA.

Discussion

In this study, we established a new HCV subgenomic 1b replicon possessing 1B-2 sequences distinct from those of Con1 [15,16], N [17], and 1B-1 [27] isolates by the transfection of a subgenomic replicon RNA library to cured cells.

To date, several sequence and functional analyses [16–18,37–42] of HCV replicons isolated from G418-resistant cell clones have demonstrated that the efficient replication of HCV replicons in cell cultures is associated with specific sequences not generally observed in vivo. These cell culture-adaptive mutations drastically increase the frequency with which replication is established in vitro and have been found to be scattered throughout the NS3–NS5B regions. However, interestingly, several adaptive mutations are clustered in the central region of NS5A, the amino terminus of the NS3 helicase domain, and at two distinct positions of the NS4B region [16–18,37–42]. Although the mechanisms governing how these mutations increase replication remain unknown, these mutations can be subdivided into at least two groups by their effects on replication efficiency and cooperativity [41]. The first group is associated with mutations in NS3 (e.g., E1202G, T1280I) that have a low impact on replication efficiency. However, these mutations enhance replication cooperatively when combined with highly adaptive mutations. The second group involves mutations in NS4B (e.g., K1846T, V1897A), NS5A (e.g., S2197P, S2204I), and NS5B (e.g., R2884G), and this group has a high impact on replication efficiency; however, these mutations are incompatible with each other [40,41]. In this study, we found that a 1B-2R1 subgenomic replicon possessed one substitution of arginine for serine at amino acid position 2200 in NS5A (S2200R), which was the same as one of the adaptive mutations reported by Lanford et al. [37]. Therefore, substitution S2200R may contribute to the establishment of a new 1B-2R1 subgenomic replicon. In addition, as a specific sequence not generally observed in vivo to date, we found that at position 4479 (the number of the nucleotide in the HCV genotype 1b genome), thymidine was exchanged for adenosine, resulting in the substitution of phenylalanine for isoleucine at amino acid position 1380 in the NS3 (I1380F). Since this position is located in the helicase domain of NS3, this unusual substitution might further enhance the efficiency of replication by its cooperative function with S2200R. However, it remains unclear whether or not the I1380F and S2200R substitutions were already present in our replicon RNA library before transfection to the cells. On the other hand, Lohmann et al. [41] recently reported that the efficiency of HCV replication in cell cultures was determined both by adaptation of the viral sequence and by the host cell itself. The use of cured cells, in which the 50-1 replicon was eliminated by IFN-α, might also be a key determinant of the successful establishment of 1B-2R1 replicon cells, as was also described in another report concerned with the genotype 1a subgenomic replicon [18]. To address these questions, further experiments will be needed.

To date, IFN has been the sole effective antiviral reagent used in the clinical treatment of hepatitis C, but its effectiveness is limited, i.e., only about one-half of all treated patients respond to therapy [43]. However, it should be noted that treatment outcome varies among the HCV genotypes. The such current status of IFN therapy suggests that the HCV encodes protein products that may directly or indirectly attenuate the antiviral actions of IFN. However, the persistence of Con1- and N-based subgenomic replicons has been shown to be sensitive to IFN-α [16,19,20,37] and IFN-γ [21,37]. In this study, we demonstrated that the 1B-2R1 and the 50-1 subgenomic replicons were sensitive to both IFN-α and IFN-γ, although the IFN sensitivities of both replicons differed slightly. In addition, we demonstrated for the first time that IFN-β also effectively suppressed the replication of HCV subgenomic RNA. Although the mechanisms by which IFNs suppress HCV replication have not yet been defined, recent studies have suggested that IFN-α may prevent HCV replication by inducing translational control programs that suppress the function of the HCV IRES [44,45]. Furthermore, a recent study [46] using a Con1-based subgenomic replicon indicated that IFN-α blocked HCV replication through translational control programs involving double-stranded RNA-activated protein kinase (PKR) and P56 to target eukaryotic initiation factor 2 (eIF2)- and eIF3-dependent steps, respectively, in the viral RNA trans-